A comparison of the performance of lumped hydrological models in modelling a flash flood in the Hupsel Brook catchment

MSc thesis

Wageningen, 14 August 2012

Peter Kloosterman

A comparison of the performance of lumped hydrological models in modelling a flash flood in the Hupsel Brook catchment

MSc thesis

A thesis submitted in partial fulfilment of the
requirements for the degree of

MASTER OF SCIENCE

By

Peter Kloosterman

Examinor: Prof. dr. ir. Remko Uijlenhoet

Supervisors: Claudia Brauer MSc

Dr. ir. Ryan Teuling

Prof. dr. ir. Remko Uijlenhoet

Hydrology and Quantitative Water Management Group
Wageningen University, Wageningen
[Picture cover: Photo courtesy by A.J. Teuling]

Preface

This report is the result of a MSc thesis for the study Hydrology and Water Quality at Wageningen University. Without the help of the following people I could not have completed this thesis.

First I would like to thank Claudia Brauer, my supervisor, for supporting me and helping me out with questions I had. She gave me all measurement data and wrote the R script of the Wageningen Model. I would also like to thank Ryan Teuling, my other supervisor, for his inspiring ideas for further research and his critical view on my results and Jos van Dam, who helped me getting experienced with the SWAP model. And finally I would like to thank Ype van der Velde, for supplying me with the model code of LGSI and answering my questions about the LGSI model.

Although everyone from the hydrology department needed to find one's niche after moving to the new workplace in the Lumen building, the work atmosphere was always relaxed and informal. Anne van Loon, Marjolein van Huijgevoort and Paul Torfs always made some time if I wanted to exchange thoughts or if I needed some help with HBV.

Table of Contents

Summary

In the Hupsel Brook catchment, a rainfall event of more than 140 mm occurred on 26 August 2010, causing floods in a large area of the catchment. In Europe, flash floods are one of the most significant natural hazards (Gaume et al., 2009). Rainfall runoff models are developed to predict the discharge caused by rainfall events. This information from models may eventually help in reducing flood damage, give out warnings and do preparation measurements. A wide range of rainfall-runoff models exists, including simple lumped conceptual models and extensive distributed physically based models. In this thesis, 5 lumped models are used to describe the discharge peak observed in the Hupsel Brook catchment on 27 August 2010 and their performance is compared.

The Hupsel Brook catchment is a freely draining lowland catchment situated in the eastern part of The Netherlands and has an area of 6.6 km^2 (Brauer et al., 2011). Land use is predominantly grassland. Measurements of precipitation, discharge, potential evapotranspiration and groundwater levels have been done in the catchment at a daily and hourly time resolution. For a short period from 14 August to 3 September, soil moisture and groundwater level data were available at a 15 minute resolution. Observed discharge started to rise on 26 August at 07:00 UTC. Peak discharge on 27 August was 42.2 mm d^{-1}, and the hourly discharge peak at 03:00 UTC was 2.8 mm h^{-1}. The runoff ratio was 0.38 and the lag time 10 hours.

The 5 hydrological models which were compared to the observed data are: Hydrologiska Byrans Vattenbalansavdelning (HBV), Wageningen Model, Sacramento Soil Moisture Accounting (SAC-SMA) model, Lowland Groundwater-Surface water Interaction (LGSI) model and Soil, Water, Atmosphere and Plant (SWAP). These models are lumped, which means that the catchment is modelled as a whole (no division in sub-catchments or grids) and that the spatial variability is accounted for by catchment averaged parameters. The first three models calculate the total discharge as the sum of the outflow of multiple linear reservoirs. LGSI and SWAP are more physically based. LGSI simulates the various flow routes observed in a catchment by a relation with the amount of water stored in the saturated zone and SWAP calculates water fluxes with physically based equations. Both the Wageningen Model and SWAP have been run with a daily and hourly time resolution, the other models only daily. Within SWAP the sensitivity of the parameters Leaf Area Index (LAI) and saturated hydraulic conductivity (K_{sat}) have been analysed.

After the models were calibrated, they were run for a period from 01 April 2010 to 01 April 2011. It was found that SWAP simulated a too high evapotranspiration flux during summer, causing groundwater levels to drop too much. An adjustment in LAI and K_{sat} resulted in better model performance (NSE = 0.769). LGSI and the Wageningen Model (hourly time resolution) resulted in the highest Nash-Sutcliffe efficiency, 0.811 and 0.821 respectively.

An event period was defined running from 14 August to 20 September. During this period the models were analysed in more detail. Discharge peaks were underestimated by all models with a daily time resolution. The Wageningen Model run with daily resolution simulated the discharge peak one day later than observed. Timing of the start of discharge increase and the discharge peak deviated a few hours for the models with an hourly resolution (Table 5.1), and peaks were overestimated. Simulated groundwater remained too long above soil surface in the SWAP model.

For water balance studies the models with hourly and daily time resolution both perform well. LGSI has the advantage of giving the contribution of each flow route which can be observed in a lowland catchment. For exact timing of discharge peaks and the start of flooding a higher time resolution is needed. The Wageningen Model with an hourly time resolution was found to be most accurate in timing the start and peak of the discharge response.

1. Introduction

The motive for this research comes from the flood on 27 August 2010 in the Hupsel Brook catchment which occurred after a rainfall event of more than 140 mm in 24 hours. Although the catchment is rather flat, the rainfall caused flooding of a large area. Because the period before the rainfall event was relatively dry, soil moisture was depleted. This caused groundwater levels to be low and the buffer to the extreme precipitation large. When extreme rainfall events would occur on catchments which are more wet, response times will be shorter and the chance on flooding larger. In Belgium and the southern parts of the Netherlands, for example, a severe rainfall event happened in 2010. A depression passed on 12 and 13 November 2010 over Belgium and Limburg, causing some major flooding in that region with a financial loss of more than 180 million euros and the death of three people (NOS, 2011). From 12 November 14:00 to 13 November 24:00 86.8 mm of rainfall was measured in Maastricht. In Schinnen and Beek a total of 97.0 and 93.0 mm was recorded on 13 and 14 November (source: KNMI). Because rainfall amounts in these regions were high the days before the event, the soil moisture reservoir had filled up, leading to low infiltration capacities and a quick discharge response.

Flash floods, as the events described above are called, are defined as extreme floods generated by intense precipitation over rapidly responding catchments (Brauer et al., 2011). Flash floods are important phenomena, in Europe flash floods are one of the most significant natural hazards (Gaume et al., 2009). Although most flash floods occur in mountainous catchments, extreme rainfall may also trigger flash floods in lowland catchments due to overland flow. Often rainfall-runoff models are designed and calibrated with less extreme discharge data and then used to forecast peak flows, but during high flows the hydrological processes in the catchment might be different than during low flows. Therefore, and also because most flash flood research up till now focused on mountainous areas, it is necessary to do more research to understand the hydrological processes and the performance of models during discharge extremes in lowland catchments (Brauer et al., 2011). The ability to describe and predict high discharge events is important. With the knowledge gained by the investigations of the hydrological processes during flash floods, rainfall-runoff models can be improved in describing peak discharges. Accurately describing the relation between rainfall and runoff will contribute to improving flood forecasts. When a model is able to predict the runoff of an intense rainfall event with a given return period, predictions, warnings, and preparation measurements in case of flooding events can be improved.

Hydrologist who want to simulate the rainfall-runoff process have a wide choice of models to choose from. Lumped conceptual models convert precipitation time series to discharge with only a few parameters, but physically based distributed models often need multiple input files and parameter sets. Setting up a very extensive three dimensional models takes more time and adding more parameters will also add more uncertainty to the model, while the increase in performance might not be significant (Beven, 1996). Considering this, a comparison of commonly used rainfall-runoff models with different model structures is valuable to gain insight in the performance of each model.

For this thesis a comparison will be made between 5 lumped models which are often used in The Netherlands for describing discharge dynamics: 4 lumped conceptual models (HBV, Wageningen Model, SAC-SMA and LGSI) and a one-dimensional vertical model (SWAP). With exception of SAC-SMA, all models have been used before at the Wageningen University in other studies (e.g. Van Loon and Van Lanen (2011), Velner et al. (2008), Van der Velde et al. (2009) and Van Dam et al. (2008)). Each researcher, however, has a preference for a specific model. The first three models use reservoirs with outflow equations to represent discharge, LGSI uses a relation with the amount of water stored in the saturated zone to simulate spatially variable discharge processes and SWAP calculates water fluxes with physically based equations. A comparison between these models, with their different model structures, gives a varied view on the performance of the models to simulate peak discharges.

The central question in this thesis is:

How well can commonly used rainfall-runoff models describe high discharge extremes in a lowland catchment like the Hupsel Brook catchment?

The following sub questions are being posed:

- What are the catchment characteristics, and what are the observed temporal discharge, precipitation, soil moisture and groundwater level dynamics of the Hupsel Brook catchment?
- Which model performs best in describing the discharge peak on 27 August 2010 in the Hupsel Brook catchment?
- How does the performance of the model relate to the structure of the model?
- How does the temporal discretization influence the model results?

2. Field site and data

2.1 Catchment characteristics

The Hupsel Brook catchment is a freely draining lowland catchment which is situated in the eastern part of The Netherlands (Figure 2.1). The catchment has an area of 6.6 km^2, surface elevations ranging from 22 to 35 m above sea level and a mean slope of 0.8 % (Brauer et al., 2011). The slope in the 4 km long brook is about 0.2 %. Seven small tributaries are present with lengths varying from 300 to 1500 m. Average water fluxes during a hydrological year are given in Table 2.1

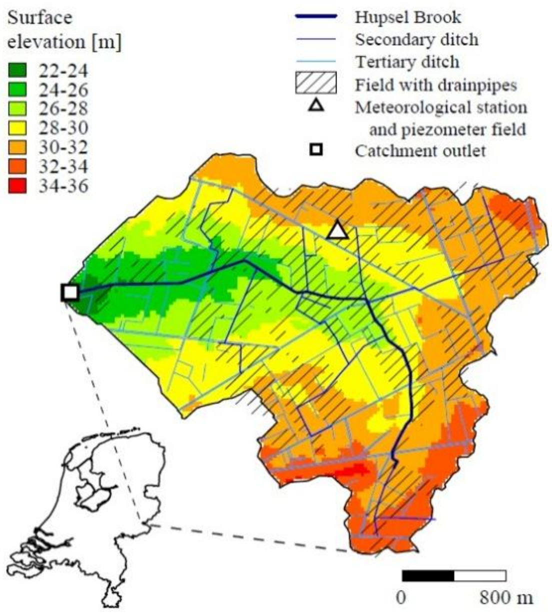

Figure 2.1 Hupsel Brook catchment with main hydrological features (Brauer et al., 2011)

An impermeable boundary for the unconfined aquifer is formed by the Miocene clay layer of approximately 20-30 m thickness (Van der Velde et al., 2009). On top of this clay layer Pleistocene aeolian sands were deposited, with some layers of clay, peat and gravel. The soil texture class is mostly loamy sand and depths of this sand layer vary from 0.5 m in the east to 20 m in the west.

The Hupsel Brook catchment has been monitored extensively for a long time. Already since the 1960s experiments have been done by Wageningen University. The combination of a small area with a thin phreatic aquifer overlying an impermeably clay layer makes the catchment well suited for hydrological studies. Water and solute balance studies can be done with good accuracy and moreover residence times are relatively short. The composition of ground- and surface water therefore reacts relatively fast on changing input signals of solutes (Eertwegh and Meinardi, 1999).

Table 2.1 Mean water fluxes, temperature and groundwater depth are calculated from complete measured data series for hydrological years (1 April to 1 April) over the period 1964-2011.

Characteristic	Value	Unit
Mean annual precipitation	801.0	mm
Mean annual discharge	297.0	mm
Mean annual potential evapotranspiration	563.1	mm
Mean annual temperature	9.9	°C

The land use is roughly 59 % grassland, 33 % agriculture (mostly maize), 3 % forest and 5 % built-on areas (Brauer et al., 2011). Because a large fraction of the land is used for agriculture, adjustments have been made to improve aeration of soils and their accessibility for machines (Lennartz et al., 2010). The number of subsurface tube drains and new ditches increased over the years. About 50 % of the fields in the catchment have presently tube drains installed. Tube drain characteristics are given in Table 2.2. These tube drains may cause increased discharge during and shortly after rainfall events, but they also lower the groundwater table, enhancing the soil storage capacity, which leads to a decrease in overland flow and discharge peaks (Skaggs et al., 1994). The average distance between the ditches is 300 m.

Table 2.2 Characteristics of the installed tube drains in the Hupsel Brook catchment (Van der Velde et al., 2009).

Tube drain characteristics	Value	Unit
Tube drain area	50	%
Drain spacing	14.5	m
Drain entrance resistance	35	d
Drain depth	0.8	m
Wet perimeter	18.84	cm

2.2 Flow routes in lowland catchments

Four major flow routes can be discerned in a freely draining lowland catchment: groundwater seepage into surface water, ponding and overland flow, tube drain flow and natural drainage by animal burrows (Van der Velde, 2011). Mostly the total discharge from a catchment is split up in a hydrological model in a quick flow component (overland flow and surface runoff), interflow component (drainage flow, subsurface runoff, macropore flow, seepage flow) and a baseflow (predominantly groundwater flow) (Willems, 2009).

Van der Velde et al. (2010) found, based on measurements done during a winter period from November through May, that, on the catchment scale, the contribution of tube drain flow was 59 % with the remaining part being overland and groundwater flow. The contribution of each individual flow route is determined by three mechanisms, which are (Van der Velde et al., 2009):

1) Dynamic area of active drainage network (streams, ditches, and tube drains). During wet conditions all tube drains and soil surface depressions generate discharge, while during dry conditions almost all streams, ditches and tube drains dry up.
2) Groundwater tables give a stronger reaction to rainfall events during wet conditions than during dry conditions, because less pores are filled with air.
3) Ponding and high surface water levels reduce discharge by reducing groundwater table gradients towards the draining ditches and surface elevation depressions. Reduced gradients lead to lower fluxes and consequently ponding and high surface water levels dampen discharge.

2.3 Data description

Daily time series of precipitation, temperature, discharge, potential evapotranspiration and groundwater levels for the Hupsel Brook catchment were available from the 1960s. Discharge is measured at the outlet of the catchment (Figure 2.1) with an H-flume, first by “Study Group Hupsel Brook” and from 2000 by Water Board Rijn and IJssel. Precipitation, temperature and global radiation were measured at the local meteorological station in Hupsel (52°04’N; 06°39'E) by “Study Group Hupsel Brook” until 1990 and afterwards by KNMI (Royal Dutch Meteorological Institute). Reference evapotranspiration (ET_{ref}) is estimated with the method of Makkink. Groundwater levels were measured by “Study Group Hupsel Brook”, WUR and Deltares. For the model comparison study, data from 9 years between 1991 and 2011 have been used. For more details about the used periods, see Section 4.1. The time series used for the model comparison study contain five missing values. The missing precipitation and temperature values on 7 and 8 May 1990 were filled up with an estimate based on measurements from the neighbouring meteorological stations (Deelen and Twente). For the gap on 6 October 1993 precipitation data was available for the first 7 hours with a sum of 0.8 mm only from the first three hours. Because discharge reached a peak on the 8th hour and declined continuously after that it is assumed after the first 7 hours no precipitation occurred.

Precipitation, discharge, potential evapotranspiration and groundwater levels were measured with an hourly resolution since 1991. There were only a few data gaps which were filled by linear interpolation. The SWAP model requires additional meteorological data when the model is run with hourly data. The model needs additional time series of solar radiation, air temperature, air humidity and wind speed to calculate the reference evapotranspiration with Penman-Monteith. The air humidity is given in percentages by the KNMI. To convert this to absolute humidity [kPa] equation [1] and [2] are used (Allen et al., 1998).

$$e_{sat} = 0.611 * e^{\left(\frac{17.27*T}{T+237.3}\right)} \quad [1]$$

$$e_{abs} = e_{rel} * e_{sat} \quad [2]$$

For the days around the flooding event on 27 August 2010, almost all groundwater level data were missing in the daily and hourly time series. To be able to compare simulated groundwater levels during the flooding event with observed data, a time series consisting of groundwater levels and soil moisture levels at a 15 minute resolution was used. These two variables were measured by WUR in a field with piezometers next to the meteorological station (Figure 2.1). For the groundwater levels the average was taken of data recorded with pressure sensors from two piezometers: one in a local elevation and one in a local depression. Soil moisture content was measured in the field with Echoprobe capacitance sensors at a depth of 40 cm. The total soil moisture storage was calculated as the depth of the unsaturated zone times the soil moisture content. Groundwater levels were available from 22 July 2010 to 3 September 2010, and soil moisture from 14 August 2010 to 3 September 2010.

2.4 Data analysis of the event

In this section the measured water fluxes in the Hupsel Brook catchment over the period 1 April 2010 to 1 April 2011 are discussed. Specifically the response of the catchment to the precipitation event around 26 August 2010 is given attention. This is done by defining an event period from 14 August 2010 to 20 September 2010 (see Figure 2.2) over which the catchment response is analysed.

The rainfall event from 26 August 04:00 to 27 August 03:00 resulted in a cumulative precipitation amount of 151.8 mm. On 26 August 142.3 mm fell in 24 hours. This corresponds with a return period of over 1000 years (Brauer et al., 2011). The total precipitation over the entire year is 867.4 mm (Table 2.3), this is 66.4

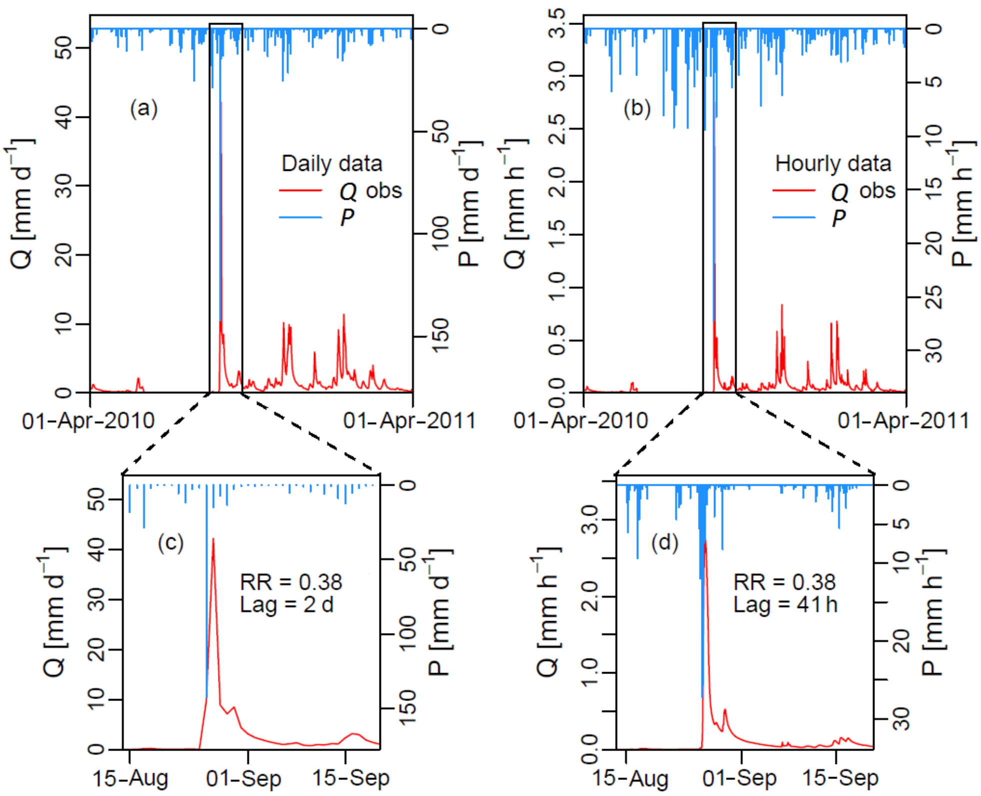

Figure 2.2 Measured precipitation and discharge time series with daily (a) and hourly (b) resolution. For the event period (c)-(d) (14 Aug - 20 Sept) the runoff ratio (RR) and lag time are given.

mm higher than the yearly average (Table 2.1). These yearly averages in Table 2.1 are calculated for the hydrological years between 1964 and 2010 which did not have missing values. During 21 of the 46 years the precipitation sum exceeded 801 mm and during 8 years 900 mm. The discharge in 2010 accumulated to 474.3 mm, which is only exceeded in the years 1993 (564.5 mm), 1994 (493.1 mm) and 1996 (644.2 mm).

Table 2.3 Total water fluxes and average temperature measured at Hupsel station from 01-04-2010 to 01-04-2011

Characteristic	Value	Unit
Precipitation (*P*)	867.4	mm
Discharge (*Q*)	474.3	mm
Potential evapotranspiration (ET_{pot})	592.6	mm
Estimated actual evapotranspiration (ET_{act})	393.1	mm
Average temperature (*T*)	9.2	°C

The total measured precipitation and discharge during the event period are given in Table 2.4 for both the daily and hourly time series. The daily peak discharge is almost twice as high as the highest discharge ever measured before in the Hupsel Brook catchment, which was 21.4 mm d^{-1} on 18 Nov 1990. The hourly discharge is more than 1.6 times as high as the highest measured hourly discharge on 31 Dec 1993 which was 1.66 mm h^{-1}. The runoff ratio (RR), calculated by dividing the cumulative discharge by the cumulative precipitation for the event period (14 August – 20 September), was found to be 0.38. Brauer et al. (2011) found for the period between 26 August and 7 September a runoff ratio of 0.5. This indicates that closer to the event of 26 August more water was transported to the outlet by direct runoff, and therefore less water evaporated or was stored in the soil. A measure of the delay is the lag time. Two of the most used definitions are: (1) time interval between the centroid of precipitation to the centroid of discharge; and (2) time interval between the centroid of effective rainfall and the peak of direct runoff (Talei and Chua, 2012). The second definition gives more insight in how fast the catchment responds and is therefore more informative for this study. The first definition was used in a study written by Hobbelt (2011), who analysed amongst other things the discharge response of the Hupsel Brook catchment. Both definitions are therefore interesting to have a look at. From here on the lag time calculated with the first definition is abbreviated as Lag 1 and the lag time calculated with the second definition as Lag 2. The calculated Lag 1 of 2 days is quite large considering that the time between start of the rainfall event (26 Aug. 04:00 UTC) and peak of the discharge response (27 Aug. 03:00 UTC) is less than one day. But because the lag time is calculated as the difference between the centroids of precipitation and discharge, increasing the end date of the event period will move the centroid of discharge to a later time due to the slowly declining tail of the discharge response. Hobbelt (2011) calculated a lag time of 24 hours over a period from

Table 2.4 Total precipitation and discharge, runoff ratio (RR) and lag time measured on a daily and hourly time scale for the period from 14-Aug-2010 to 20-Sept-2011.

Characteristic	Daily data		Hourly data	
P sum	297.9	mm	297.9	mm
Q sum	114.2	mm	114.2	mm
Q peak	42.2	mm d^{-1}	2.8	mm h^{-1}
RR	0.38	-	0.38	-
Lag 1	2	d	41	h
Lag 2	1	d	10	h
Start rising limb	25-Aug-2010		26-Aug-2010 07:00 UTC	
Date *Q* peak	27-Aug-2010		27-Aug-2010 03:00 UTC	

25 August to 7 September and found the centroid of discharge to be on 27 August 16:00 UTC. In this study the centroid of discharge was found to be on 28 August 10:00 UTC. The longer declining discharge tail is responsible for the higher lag time compared to what was found by Hobbelt (2011).

Measured time series of discharge, soil moisture content and groundwater levels are given in Figure 2.3. The measured volumetric soil water content might be difficult to compare to simulated soil moisture levels in rainfall runoff models. Often models either use a reservoir with a fixed volume to simulate total soil moisture storage, or calculate the soil moisture storage in an unsaturated zone with variable thickness. Neither of these model structures compares to the measured soil moisture content at one depth. A comparison between measured soil moisture content and simulated soil moisture stored in the unsaturated zone could be made with two assumptions. The first assumption is that soil moisture storage in the unsaturated zone can be calculated as the soil moisture content (at 40 cm depth) times the depth of the groundwater level. The second

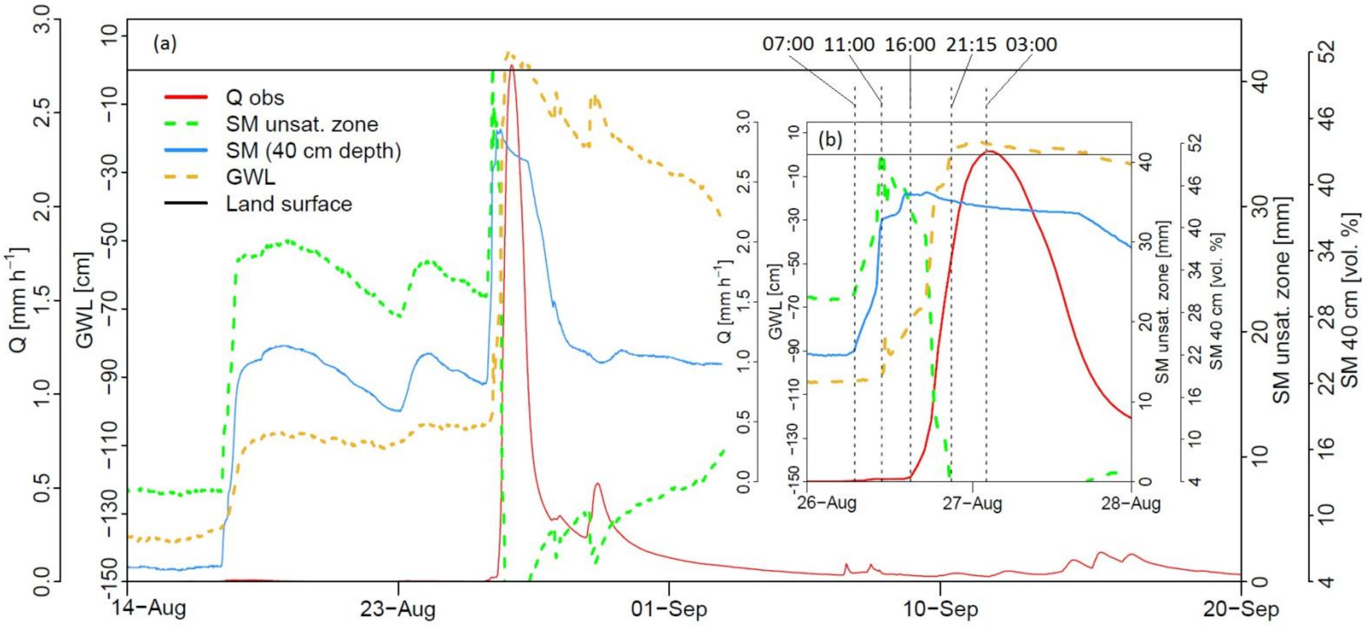

Figure 2.3 (a) Time series of discharge, soil moisture (SM) and groundwater level (GWL) measured during the event period from 14 August to 20 September. (b) With dashed lines the start of the rising limb of respectively SM (07:00), discharge (07:00) and GWL (11:00) is given. At 16:00 the most spectacular rise of discharge occurred. The dashed line at 21:15 is the time of ponding and the line at 03:00 the time of the discharge peak.

assumption is that the shape of the simulated response curve of soil moisture storage in a reservoir, is comparable to the shape of the response curve of the measured volumetric soil moisture content at one depth. The main problem with both assumptions is that the response of soil moisture is very variable in the vertical direction. While tops soil might be saturated after a rainfall event for example, the rise of soil moisture content deeper in the profile might occur much later. The specific response of discharge, soil moisture and groundwater level during two days around the event shows more clearly how each variable reacts to the precipitation event (Figure 2.3b). The precipitation event started on 26 August at 04:00 UTC and continued to 03:00 UTC on 27 August. Soil moisture began to rise 3 hours after the start of precipitation. Discharge also showed at this time a small increase, but at 16:00 UTC discharge rose rapidly to peak at 03:00 UTC the next day. Groundwater levels started to rise at 11:00 UTC and reached land surface at 21:15 UTC. Although discharge began to rise at 07:00 UTC already, the fasted increase started 9 hours later. At 16:00 UTC the groundwater level (-73 cm) was above most tube drains and the soil was saturated (45 %). This increased the area of the active drainage network. Fast flow routes then could cause a fast increase of discharge.

3. Description of the hydrological models

There are many well-known models which are used to simulate rainfall-runoff processes. For this model comparison study 5 models were chosen: Hydrologiska Byrans Vattenbalansavdelning (HBV), Wageningen Model, Sacramento Soil Moisture Accounting (SAC-SMA) model, Lowland Groundwater-Surface water Interaction (LGSI) model and Soil, Water, Atmosphere and Plant (SWAP). All 5 models are lumped. With lumping the catchment is modelled as a whole (no division in sub-catchments or grids) and it is assumed that the spatial variability is accounted for by catchment averaged parameters. The first three models calculate the total discharge as the sum of the outflow of multiple linear reservoirs. LGSI and SWAP are more physically based. LGSI simulates the various flow routes observed in a catchment by a relation with the amount of water stored in the saturated zone and SWAP calculates water fluxes with physically based equations.

3.1 Hydrologiska Byrans Vattenbalansavdelning (HBV)

3.1.1 Theory

The first version of the HBV model was developed at the Swedish Meteorological and Hydrological Institute (SMHI) by Sten Bergström in the 1970s. For this thesis HBV-light version 2.0 is used. HBV-light (Seibert, 1997) is a user-friendly Windows version and has basic equations in accordance to the SMHI version HBV-6 with only two slight changes. The standard HBV-light model has 16 parameters and consists of a snow routine, soil routine, response function and routing routine (Figure 3.1 Basic structure HBV light). The snow and soil routine can be distributed and divided into elevation and vegetation zones, but for this research the catchment parameters are averaged for the whole catchment.

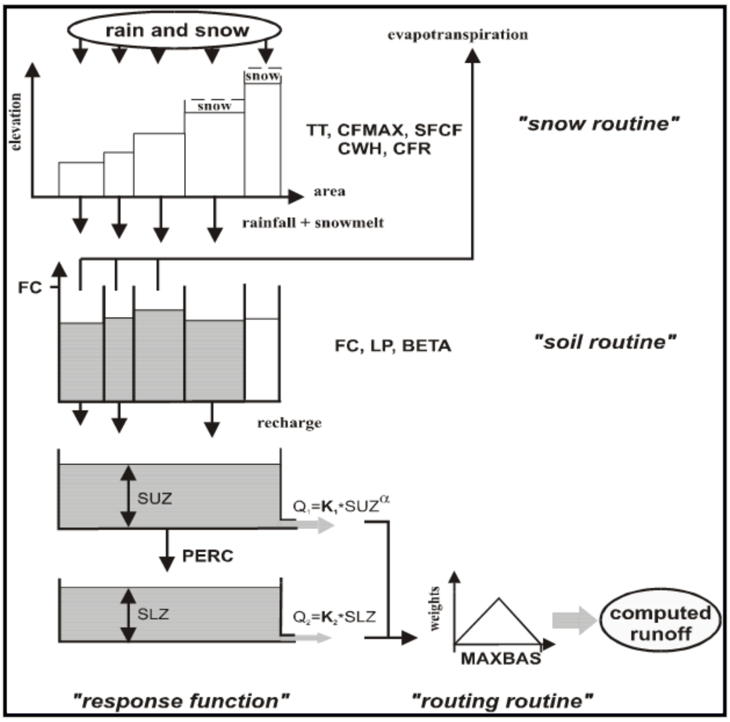

Figure 3.1 Basic structure HBV light (Seibert, 2000).

To determine if precipitation falls as snow or rain a threshold temperature is introduced (TT). The precipitation which falls as snow is multiplied with a correction factor (SFCF). The amount of snow melt is calculated by multiplying the positive temperature difference (T-TT) with a degree-day factor (CFMAX). The snowmelt and rainfall are retained in the snowpack until the total exceeds the water holding capacity (CWH). Refreezing of the liquid water occurs according to the coefficient CFR. The shape factor BETA and the ratio of actual soil moisture content (SM(t)) and maximum soil moisture storage (FC) in the soil routine determine the amount of water from precipitation and snowmelt stored in the soil and the amount which goes to the response function as groundwater recharge. The actual evaporation is calculated with an evaporation threshold LP. When the ratio SM(t)/FC is above LP the actual evaporation equals the potential evaporation, otherwise a linear reduction function is used. In the response function an upper and lower reservoir exist, representing the upper and lower groundwater zones. Eight model structures can be chosen for the response function; these include distributed models, more than one groundwater box or a different delay function in the response routine. The lower reservoir is filled with percolated water from the upper zone depending on the percolation rate PERC. With linear reservoir equations the outflow of these boxes is calculated. The outflow of the reservoirs of one time step is converted to simulated runoff over the next time steps (days) by the routing routine with a triangular weighting function defined by the parameter MAXBAS. Besides the 13 parameters needed in the model with the standard response function three parameters for conversion of input data exist if you use the model with different elevation zones or monthly mean potential evapotranspiration input data. Because the Hupsel Brook catchment is flat, small and fast responding, the standard model with use of threshold UZL and recession coefficient K0 in the Storage Upper Zone (SUZ) box is chosen as response function (Figure 3.2). The SUZ box has in this structure two linear reservoir equations. The recession coefficients K_0 and K_1 multiplied by the storage in SUZ represents peak (Q0) and intermediate flow (Q1) respectively. The outflow of the lower groundwater box (SLZ) represents the base flow (Q2) and depends on K_2.

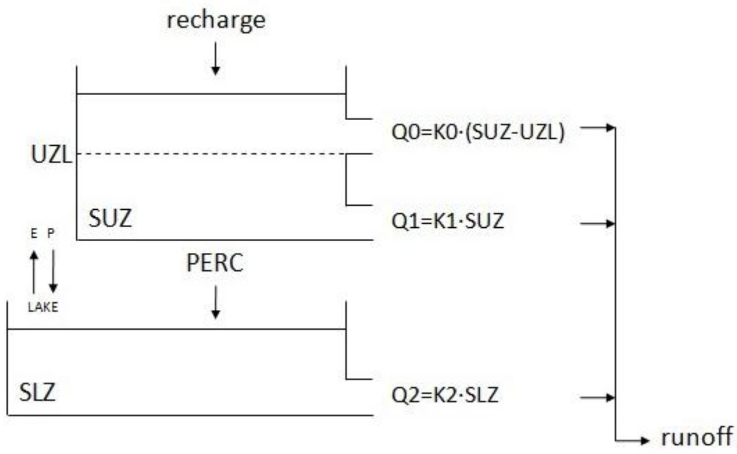

Figure 3.2 Standard Model structure for response function with use of threshold UZL and coefficient K0 (Seibert, 2000).

3.1.2 Implementation and data description

In the model used in this thesis a total of 14 model parameters were needed. Parameter ranges (Table 4.2) are taken from Seibert (1997, 1999, 2000). These ranges are broad enough to be also applicable to the Hupsel Brook catchment. To run the model, three data files are necessary. The first file contains daily precipitation (mm d^{-1}), temperature (°C) and discharge time series (mm d^{-1}). The second file contains a time series of potential evapotranspiration, which might cover the same period as the first file or be monthly values. For this study daily evapotranspiration values have been used. The third file contains the parameter values (after the model has been calibrated).

Table 3.1 Parameter ranges for HBV model

Parameter	Minimum	Maximum	Unit
TT	-1.5	2.5	°C
CFMAX	1	10	mm $°C^{-1}$ d^{-1}
SFCF	0.5	1.2	-
CFR	0	0.1	-
CWH	0	0.2	-
FC	50	500	mm
LP	0.3	1	-
BETA	1	6	-
PERC	0	4	mm d^{-1}
UZL	0	50	mm
K0	0.1	0.5	d^{-1}
K1	0.05	0.3	d^{-1}
K2	0.001	0.1	d^{-1}
MAXBAS	1	7	d

To obtain a set of parameters, different automatic calibration methods are implemented in the HBV model itself. Seven objective functions can be used for the optimization. For this study the Nash-Sutcliffe efficiency (R_{eff}) has been used as objective function for calibrating on discharge data. The total of 5000 model runs was divided into 3800 runs for the genetic algorithm and 1200 runs for a subsequent local optimization. Powell's quadratically convergent method is used for the subsequent local optimization within HBV. By using multiple populations, which each calibrate the model with the objective function, genetic algorithms can be improved (Whitley, 1994;Punch, 1998). The total number of populations has been set to 4. When more than one optimum set of parameter values exists it is possible to select the one which gives the best efficiency.

3.2 Wageningen Model

3.2.1 Theory

The Wageningen Model (Stricker and Warmerdam, 1982), abbreviated Wag., is developed by the hydrology department of Wageningen University in the 1980's. The model simulates the rainfall-runoff process by keeping water balances of a soil moisture reservoir, a groundwater reservoir and an open water reservoir. It only needs 11 parameters, but in contrast to HBV it is not able to model snow melt. In (Figure 3.3) the various compartments and fluxes in the model are indicated. The actual evapotranspiration is calculated with the soil moisture content. When the soil moisture content is below field capacity (FC) capillary rise occurs according the parameter FOS from the groundwater reservoir towards the soil moisture reservoir (Metselaar et al., 2011). Percolation occurs according the parameter REPA, when the soil moisture content is above field capacity and when soil moisture is above saturation (SAT) surface runoff occurs. The water which percolates is divided between a slow (groundwater) and fast (open water) reservoir with Ks and Kf as reservoir coefficient respectively. The water is divided with a formula with the parameter CR. Before the model can be run four parameters are introduced to set some initial values. SM0 gives the initial soil moisture content, Gstore0 the initial water in the groundwater reservoir, and Q_slow0 and Q_fast0 as initial discharge for the slow and fast reservoir respectively.

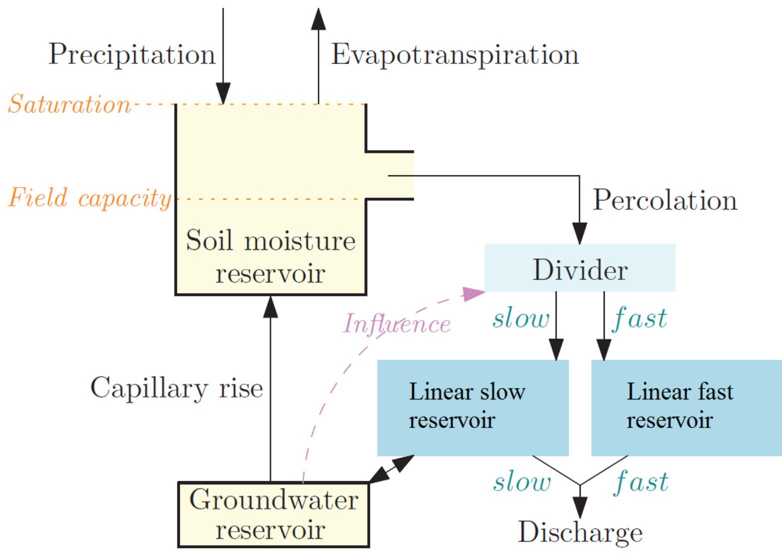

Figure 3.3 Model structure Wageningen Model (Metselaar et al., 2011).

3.2.2 Implementation and data description

The Wageningen Model needs time series of precipitation, potential evapotranspiration and discharge. In Table 4.3 the initial values and ranges of the 11 parameters are given. The Wageningen Model uses this initial value to calculate water fluxes throughout the whole five year period running from 01-April-1990 to 01-April-1995. Then it calculates the efficiency for the last four years cutting of the first year as the warming up period (Figure 4.4). This method is slightly different than the warming up method in HBV and SAC-SMA, where the initial value is solely determined by calibrating on the first year.

Table 3.2 Parameter values

Parameter	Initial value (0 %)	Lower	Upper	Unit
FC	90	50	150	mm
SAT	220	50	300	mm
REPA	0.9	0.3	1.2	-
FOS	0.5	0.1	5	mm d^{-2}
CR	5	1	10	mm^{-1}
Kf	0.5	0.1	4	d
Ks	50	50	300	d
SM0	120	10	300	mm
Gstore0	40	20	100	mm
Q_slow0	0.2	0	5	mm d^{-1}
Q_fast0	0	0	5	mm d^{-1}

By specifying one starting value for each parameter the model might calibrate towards one specific optimum on the response surface of the objective function when the model is calibrated multiple times. This could result in a set of parameters which does not give the highest value of the objective function. To get insight in the influence of different starting values on the final efficiency of the model a parameter range between -5% to 5% compared to the original starting value was given to the model. From some random tries in this range the model was finally run with four initial parameter sets. These parameter sets were -1%, 0%, +1% and +2.5% compared to the initial values mentioned in Table 4.3.

To investigate the influence of the time discretization of the model on the goodness of fit of the final simulated discharge the model was run both with daily and hourly data. For the hourly data two different scenarios were made. In the first scenario, called constant (abr. C), the four calibrated parameter value sets from the daily time discretization were converted to hourly parameter values and given to the model for the simulation period (2010-2011). In the second scenario the model was calibrated on hourly data with the initial four daily parameter value sets, which were first converted to hourly parameter values. Peaks with a short duration in the hourly time series might be averaged out in the daily time series. Because conceptual models work often with threshold values this means the response of the catchment will not be modelled correctly. Peaks in discharge will often be underestimated. With the formulation of the two scenarios it is possible to look at the effect of keeping the thresholds constant and changing the time discretization (scenario 1), compared to changing the threshold values and changing the time discretization (scenario 2).

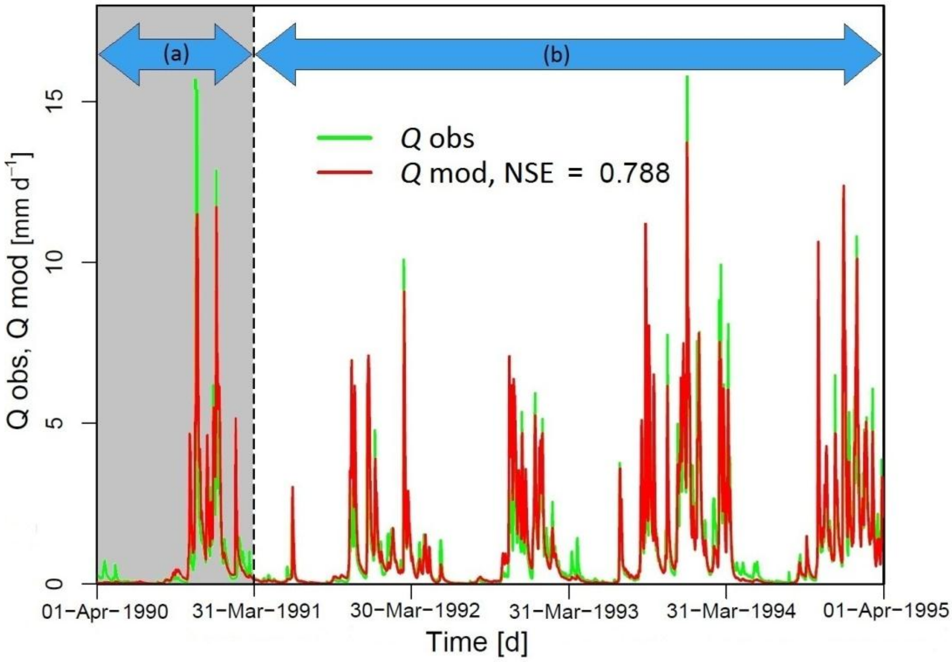

Figure 3.4 Calibration strategy of the Wageningen Model. The model calculates water fluxes during 5 years and calculates the efficiency of the last four years (b) excluding the first year as a warming up period (a).

The calibration of the model has been done with the L-BFGS-B algorithm which can be called in R's optim general purpose optimizer. The L-BFGS-B algorithm (Byrd et al., 1995) is a variant of L-BFGS algorithm which allows the use of box constraints. Recently a refinement to the subspace minimization phase and to the estimation of machine accuracy (dpmeps routine) has been made to the L-BFGS-B algorithm, this made a significant improvement to the algorithms performance (Morales and Nocedal, 2011).

3.3 Sacramento Soil Moisture Accounting model (SAC-SMA)

3.3.1 Theory

The Sacramento model (Burnash, 1995) is a soil moisture accounting model and is often abbreviated as SAC-SMA . SAC-SMA is developed by the National Weather Service in the 1970s and is used frequently by the 13 river forecasting centres throughout the United States. The model needs 13 parameters and is based on the water balance given in equation [1]:

Runoff = Rainfall – Evapotranspiration – Changes in Soil Moisture [1]

The soil profile in the SAC-SMA model is conceptualised as a series of reservoirs. The model divides the soil column in an upper and lower zone (Figure 3.5). For the soil moisture part, hygroscopic, tension and free water are the three basic types of soil moisture which can potentially influence catchment runoff. Hygroscopic water is bound very tightly to the soil molecules making it unavailable to plants. Variations in hygroscopic water are small making its influence in a rainfall-runoff model not significant. Therefore changes in the volume of hygroscopic water are a portion of the tension water within SAC-SMA. Another simplification is the inclusion of intercepted precipitation in the tension water of the upper zone. Tension water can be moved to the atmosphere by plant uptake or atmospheric forces. By molecular attraction between the soil particles and water molecules the tension water is held in position. Free water can, as the name indicates, move through the soil freely. The upper and lower zone of the soil column each have a tension and free water store. The lower zone makes also a distinction between a primary and supplementary free water store.

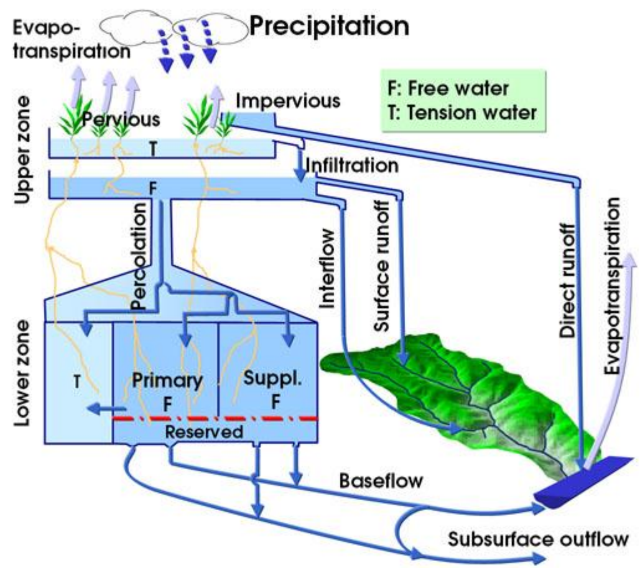

Figure 3.5 Schematization of the SAC-MSA model (CHRS, 2011)

The soil surface is divided in a permeable (pervious) area and an impermeable (impervious) area. The area which is impervious depends on the saturation of the soil, the area which is always impervious is defined by the parameter PCTIM and the additional fraction which is impervious under wet conditions is defined by the parameter ADIMP. The total potential impervious area is given by POTIM, which is the sum of PCTIM and ADIMP. The area which is actually impervious is given by the variable ACTIM and multiplied with the precipitation amount it gives the direct runoff. Surface runoff takes place over the areas which are actually pervious when precipitation occurs at a faster rate than percolation and interflow (rainfall excess) under conditions where the upper storages are full. Lateral drainage rates from the upper zone free zone is given by the parameter UZK. Interflow is given by the area which is always pervious (1-POTIM) times the lateral drainage rate, times the current water content in the upper zone free water storage (UZFWC). The maximum capacity in the upper zone of tension water is given by the parameter UZTWM and the maximum capacity of free water by UZFWM. Current contents are given by the variables UZTWC and UZFWC respectively. The maximum percolation rate coefficient is given by the parameter ZPERC and the change of percolation rate with change in lower soil moisture water contents is given by REXP. The fraction of direct percolation which goes to the lower free water zone is defined by the parameter PFREE. The lower tension water zone has a maximum water capacity defined by the parameter LZTWM and an actual content defined by LZTWC. The lower supplemental free water zone has a maximal capacity of LZFSM, a current content LZFSC and a lateral drainage rate of LZSK. And the lower primary free water zone has a maximal capacity of LZFPM, a current content LZFPC and a lateral drainage rate given by the parameter LZPK. Outflow of this lower free zone consists of a primary and supplemental base flow. With a routing model the sum of the five basic runoff forms can be converted to stream flow. Evapotranspiration in the model is calculated by multiplying the evapotranspiration series with the factor ETMULT. In this study a value of 1 is used for ETMULT, which implies the values in the input time series of evapotranspiration are used.

3.3.2 Implementation and data description

The SAC-SMA model concept is implemented in a package intended for the R environment called Hydromad (Andrews et al., 2011). The version used in this thesis is Hydromad 0.9-13. In this package also other dynamic, spatially aggregated conceptual or statistical hydrological models are included. The modelling framework may consist of two components; a soil moisture accounting model (SMA) and a routing model

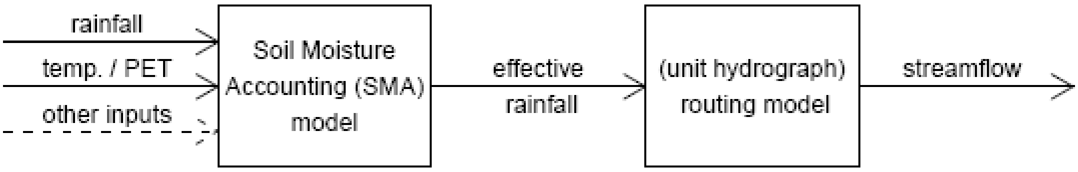

Figure 3.6 Hydromad modelling framework (Andrews,2011)

(Figure 3.6 Hydromad modelling framework). The routing module is optional and converts the output of the SMA model, the effective rainfall, to streamflow. In this thesis no routing module has been used, because that would not follow the lines of the original SAC-SMA model structure. Not using a routing module also gives the advantage of a much faster converging model. Input of the SMA model includes precipitation and evapotranspiration (or temperature) time series on a daily time scale. Because the model was set up for larger catchments (>1000 km^2) the model was not designed for hourly input data. Before the calibration starts a one year warming up period is used. The model is calibrated by the fitByOptim function, which calls the general purpose optimizer within R, and the L-BFGS-B algorithm is used to search the response surface of the objective function. The ranges of the parameters in the model are given in Table 3.3.

Table 3.3 Parameter ranges Sacramento model

Parameter	Lower	Upper	Unit
UZTWM	1	150	mm
UZFWM	1	150	mm
UZK	0.1	0.5	d^{-1}
PCTIM	0.000001	0.1	-
ADIMP	0	0.4	-
ZPERC	1	250	-
REXP	0	5	-
LZTWM	1	500	mm
LZFSM	1	1000	mm
LSFPM	1	1000	mm
LZSK	0.01	0.25	d^{-1}
LZPK	0.0001	0.25	d^{-1}
PFREE	0	0.6	-

3.4 Lowland Groundwater Surface water Interaction model (LGSI)

3.4.1 Theory

LGSI (Van der Velde et al., 2009) is a lumped hydrological model which uses 17 model parameters. LGSI has a more physical approach than the three models mentioned before because it takes into account the four individual flow routes in lowland catchments (see Chapter 2.1). The concepts are based on results of MODFLOW simulations which were run with a great spatial detail. In this way the explanatory power of a highly detailed MODFLOW model is combined with a lumped conceptual model (Van der Velde, 2011).

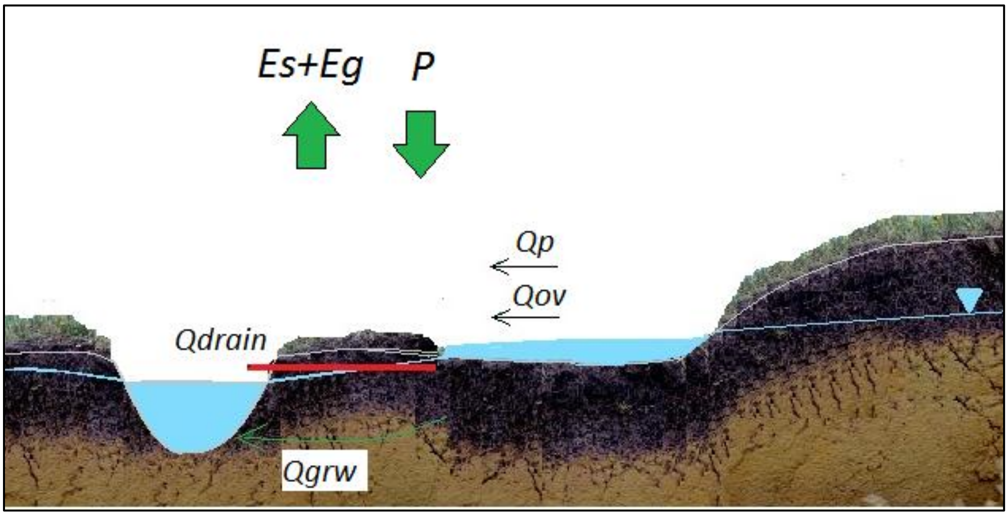

Figure 3.7 Overview of flow routes in the LGSI model. The contribution of evaporation from groundwater (*E*g), evaporation from surface water (*E*s), groundwater flow (*Q*grw), drain discharge (*Q*drain), overland flow (*Q*ov) and discharge from inundated areas (*Q*p) is based on the groundwater distribution calculated by a relation with the amount of water in the saturated zone.

The model accounts for the three hydrological mechanisms which determine the contribution of each flow route (see Chapter 2.1) by a unique relation with the amount of water in the saturated zone. Van der Velde et al. (2009) found that the spatial distribution of the groundwater depths can be approximated by a normal distribution with the mean and variance being unique functions of the amount of water stored in the saturated zone. With this relation between groundwater storage and the spatial probability distribution of groundwater depths the effects of spatial heterogeneity in soil properties, vegetation, and drainage network are lumped. The model is based on a water balance of the saturated zone, unsaturated zone and surface storage. Every term in the water balance at any given time is considered a function of the groundwater depth distribution at that time. This spatial structure of the groundwater is assumed to be scale-specific, which means that it determines the discharge from a certain flow route at a certain scale. To construct the LGSI model measurements were done at a field site in the Hupsel Brook catchment. To scale this field site measurements up to the entire catchment the spatial structure of the groundwater table for each scale (i.e. the relation between storage and the distribution of groundwater depths) was quantified (Van der Velde et al., 2011). It was found that a LGSI model of which the parameter are conditioned on nested-scale measurements much better predicted extreme discharges and nutrient loads than a LGSI-model that is constructed on catchment-discharge only. The specific volumes of the flow routes measured at the field site cannot be scaled up to the catchment scale, but the typical reaction of a flow route to rainfall events can. The typical reaction of each flow route is quantified by the process-specific parameters in the LGSI model, which were assumed scale invariant.

The dynamic surface water network concept implemented in the model makes sure that the discharge dynamics due to variable travel path lengths and variable head gradients is taken account for (Van der Velde et al., 2009). The unsaturated zone storage accounting is important to describe the dynamic interaction between groundwater and surface water. In flat lowland catchments with dynamic and shallow groundwater levels the total draining area ($A_{q,i}$) varies strongly in time. Taking a single characteristic travel path, travel time distribution, unit hydrograph or linear reservoir to model discharge and solute transport will not give a realistic representation of this dynamic behaviour. Most lumped models use fast- and slow reservoirs to describe varying discharge characteristics but these concepts do not fully recognize the dynamics in draining area and its parameters cannot be directly linked to observable catchment properties.

The water fluxes in the LGSI model are calculated based on the unique relation with the amount of water stored in the saturated zone. A change in saturated groundwater storage in the model is simplified by expressing it as a change in thickness (total pore volume) of the unsaturated zone (u[L]). The unsaturated storage is expressed as the remaining pore volume in the unsaturated zone. A good estimate for the total pore volume in the catchment is 1100 mm. The storage in the saturated zone is this total storage (1100 mm) minus the total pore volume in the unsaturated zone (named saturated storage). The storage in the unsaturated zone is the saturated storage minus the unsaturated storage. The total discharge is calculated as the sum of groundwater flow (Qgrw), overland flow (Qov), tube drain flow (Qdrain) and discharge from inundated (Qp) areas minus evaporation from surface water (Es).

3.4.2 Implementation and data description

Multiple sets of model parameters were made available by (Van der Velde et al., 2009). These parameter were calibrated on hourly discharge data, hourly measured groundwater depths and an estimated yearly 59% contribution of tube drains to the total discharge for the period 1 January 1994 to 1 January 1996. Four randomly chosen sets were used to run the model (Table 4.4).

Table 3.4 Parameter values used for each run. The names for the parameters are given as used in the model code, the names between brackets are as used in (Van der Velde et al., 2009) .

Parameter		Run 1	Run 2	Run 3	Run 4	Unit
alp	(a)	1.604	1.252	1.543	1.345	m-1
n	(n)	1.940	3.039	2.241	2.679	-
maxsd	(σ_{max})	0.662	0.399	0.446	0.668	m
minsd	(σ_{min})	0.296	0.288	0.253	0.299	m
Nb	(b)	0.252	0.347	0.257	0.286	m
Nusdmax	(u_{sdmax})	0.313	0.366	0.273	0.352	m
Rex	(r_{grw})	3.046	4.601	9.420	3.785	d
Rov	(r_{grw})	3.046	4.601	9.420	3.785	d
Ddr	(d^*_{dr})	0.797	0.763	0.759	0.810	m
Tets	(θ_s)	0.357	0.387	0.357	0.422	-
Fm	(u_{et})	1.381	1.287	1.317	1.254	m
AdrL	(g*)	0.481	0.530	0.517	0.524	-
AsdL	($A_{nd,wet}/A$)	0.010	0.009	0.010	0.011	-
As	($A_{nd,wet}/A$)	0.010	0.009	0.010	0.011	-
Atot	(A)	6281616	6088304	6138075	6074334	m^2
m	(m)	0.470	0.219	0.217	0.417	-
rdr	(r^*_{dr})	262.085	281.477	167.238	271.701	d
ml	(-)	1.609	1.609	1.609	1.609	
sdl	(-)	0.472	0.472	0.472	0.472	

3.5 Soil, Water, Atmosphere and Plant (SWAP)

3.5.1 Theory

SWAP (Van Dam, 2000) is a model which calculates fluxes of water, solutes and heat in the vadose zone with the use of physically based equations. The model is a successor of the agrohydrological model SWATR (Feddes et al., 1978) and is developed by Alterra and Wageningen University. The domain of the model runs from the top of the canopy into the groundwater. The main domains in the model are plant, pond, surface water and soil. Between these compartments various fluxes are calculated (Figure 3.8).

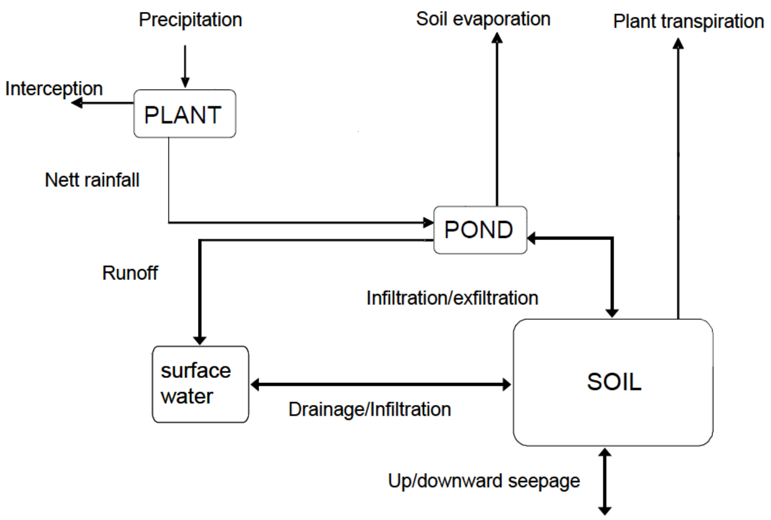

Figure 3.8 Water fluxes between the subdomains plant, pond, surface water and soil (Van Dam, 2000).

With the Richards equation and root water extraction the movement of soil moisture is described. The Muelem-Van Genuchten soil hydraulic functions are used for the soil water movement. The water balance of the ponding reservoir is given by:

$$\frac{\Delta h_0}{\Delta t} = q_{prec} + q_1 - q_{e,pond} - q_{runoff} \qquad [1]$$

Where:

$\frac{\Delta h_0}{\Delta t}$	Storage change of the ponding reservoir	[cm d^{-1}]
q_{prec}	Nett precipitation flux	[cm d^{-1}]
q_1	Flux from first soil compartment to ponding layer	[cm d^{-1}]
$q_{e,pond}$	Evaporation flux from ponding layer	[cm d^{-1}]
q_{runoff}	Surface runoff flux	[cm d^{-1}]

Surface runoff occurs when the ponding layer exceeds the critical depth $h_{0,threshold}$ [cm]:

$$q_{runoff} = \frac{1}{\gamma}(\max(0, (h_0 - h_{0,threshold}))^{\beta} \qquad [2]$$

Where:

γ	Overland flow resistance	[$cm^{\beta-1}$ d]
β	Exponent in empirical relation	[-]

3.5.2 Implementation and data description

For this thesis SWAP version 3.2.36 is used. Compared to earlier releases this version incorporates macropore flow, has better numerical stability and allows input of detailed rainfall and evapotranspiration.

The model has been run with a daily and hourly time step to investigate the influence of a different time discretization on model results. For the daily time step precipitation and reference evapotranspiration are used as input. Because SWAP does not read in evapotranspiration values in case of multiple records per day, the model needs additional time series of solar radiation, air temperature, air humidity and wind speed in case of the hourly time step to calculate the reference evapotranspiration with Penman Monteith. No heat flow (snow and frost), macropore flow, soil factor (for adjustment calculation E_{pot} from ET_{ref}), hysteresis of soil water retention function or irrigation practice has been simulated. SWAP is physically based making most of the parameters physically measurable. The 61 model parameters values are given in Appendix B. The parameters are based on the values for the Hupsel Brook catchment given by (Kroes et al., 2008). In contrast to the other models the parameters in the SWAP model cannot be calibrated automatically. For the run with hourly data the same parameters can be used because they should not depend on the temporal resolution.

Drainage in the catchment was modelled with Hooghoudt and Ernst. Total outflow was calculated by the average outflow of two model runs: one run with a catchment with tube drains and one run with a catchment with ditches. This agrees with the finding of Van der Velde et al. (2009) that about 50 % of the catchment has tube drains installed. The characteristics of the tube drains are used as given in Table 2.2. Ditches were separated 300 m apart and had an entry resistance of 20 days. The subsoil is schematised as given in Figure 3.9.

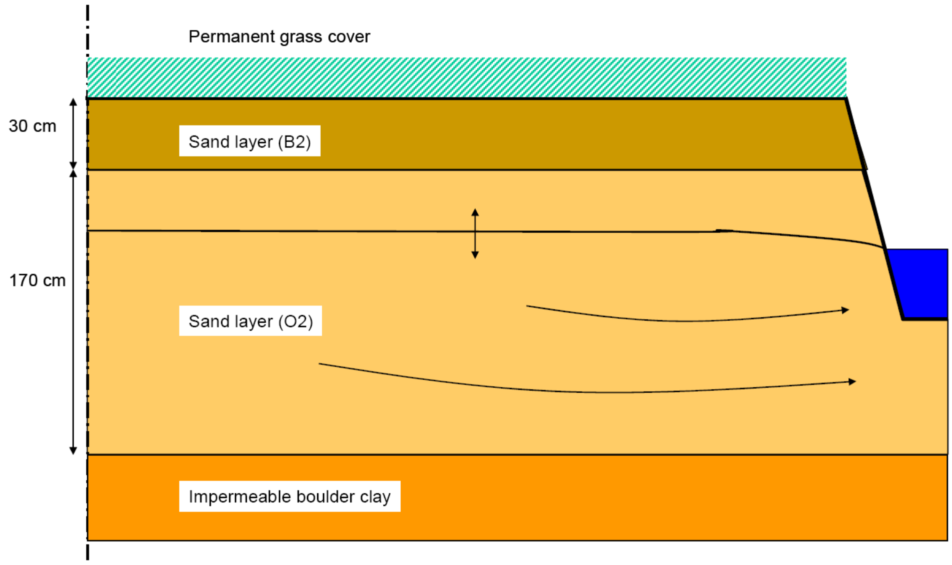

Figure 3.9 Simplified soil profile of soil layers in the Hupsel Brook catchment as used in the SWAP model.

Runoff from the soil surface occurs if the ponding layer exceeds a critical depth ($h_{0,threshold}$) of 0.2 cm. The overland flow resistance (γ) is set to 0.5 d. The total depth of the soil profile is 2 meters with a top soil of 30 cm. An impermeable (no flux) clay layer is specified as a bottom boundary. The parameter values for the soil hydraulic functions were used according to (Wösten et al., 1994). These values were also used by Kroes et al. (2008) for the example case "Hupsel". The saturated hydraulic conductivity of 9.65 cm d^{-1} as used by Kroes et al. (2008) applies to a loamy top soil (class B2). When is assumed less clay and silt is present in the top soil infiltration rates will go up. To investigate the influence of a larger infiltration flux the saturated conductivity of the top soil has been altered by assuming the top soil falls into class B1 with K_{sat} = 23.41 cm d^{-1} (Wösten et al., 2001).

Within SWAP a specific crop type must be chosen to model the interaction between the soil and atmosphere. Only one crop type per time period can be chosen, which means no spatial variation can be implemented. Because the Hupsel Brook catchment consists predominantly of grassland (59 %), during the whole simulation period the crop type has been set to grass. Grass roots are present in the whole 30 cm of the top zone. The evapotranspiration of this vegetated surface is calculated as the sum of the intercepted water, the soil evaporation and the transpiration via the stomata of a leaf. Interception water is simulated with the relation of Von Hoyningen-Huene (1983) and Braden (1985).

The Makkink reference evapotranspiration (ET_{ref}) which is given to the model must be multiplied with a crop factor to give the potential evapotranspiration (ET_{pot}). The crop factors calculated by Feddes (1987) are given in Table 4.1 for every decade of a month. The numbers I, II and III in Table 4.1 indicate the decades, where I= day 1-10, II = day 11-20 and III = day 21-last day of the month. For the winter period (October-March) a crop factor of 1.0 is used. Reduction of the potential soil evaporation is done according to the maximum Darcy flux and the maximum of the relation of Black et al. (1969).

Table 3.5 Crop factors for use with Makkink reference evapotranspiration

Month	**April**			**May**			**June**			**July**			**August**			**September**		
Decade	I	II	III	I	II	III	I	II	III	I	II	III	I	II	III	I	II	III
Grass	1.0	1.0	1.0	1.0	1.0	1.0	1.0	1.0	1.0	1.0	1.0	1.0	1.0	1.0	0.9	0.9	0.9	0.9

The amount of actual evapotranspiration was very high when all parameters were set in SWAP. Compared to the potential evapotranspiration (592.6 mm) the actual evapotranspiration was only 6 % lower (557 mm) during simulation runs. Normal evapotranspiration values for a hydrological year are on average 450 mm y^{-1} (Van der Velde et al., 2009). Runs with other models resulted also in lower actual evapotranspiration values (on average 410.56 mm). When the evapotranspiration is high, ground water levels will fall down very quickly, resulting in a very weak discharge response to the precipitation event.

To have a more realistic representation of evapotranspiration not the standard constant LAI value in SWAP has been used but an adjusted monthly varying value (Figure 3.10). Reducing the leaf area will also reduce the amount of water transpired. Other variables had such a strong physical base that adjusting them to give acceptable evapotranspiration values resulted in unrealistic parameter values. Based on measurements done at Cabauw in the Netherlands (51°58’N, 4°56’E) for the year 1987, Chen et al. (1997) formulated a time series representing the LAI of a large grass field. Not many publications are available describing the variation of the LAI during a complete year, which makes this publication very valuable. Not only were the measurements done in the same country (less than 120 km apart), the Cabauw site also consist predominantly of grassland, like the Hupsel Brook catchment. Using this time series resulted in better model performance, but still the evapotranspiration values during summer were too high and during winter too low. Therefore for this study a monthly varying LAI series based on Chen et al. (1997) has been made, with lower LAI values from May to August. When the grass is undisturbed it is however most likely LAI will be high during summer, and lower during winter. In the field these lower LAI values during the summer months could be explained as caused by mowing activities. For every month it was analysed if a slight increase or reduction in LAI would increase model

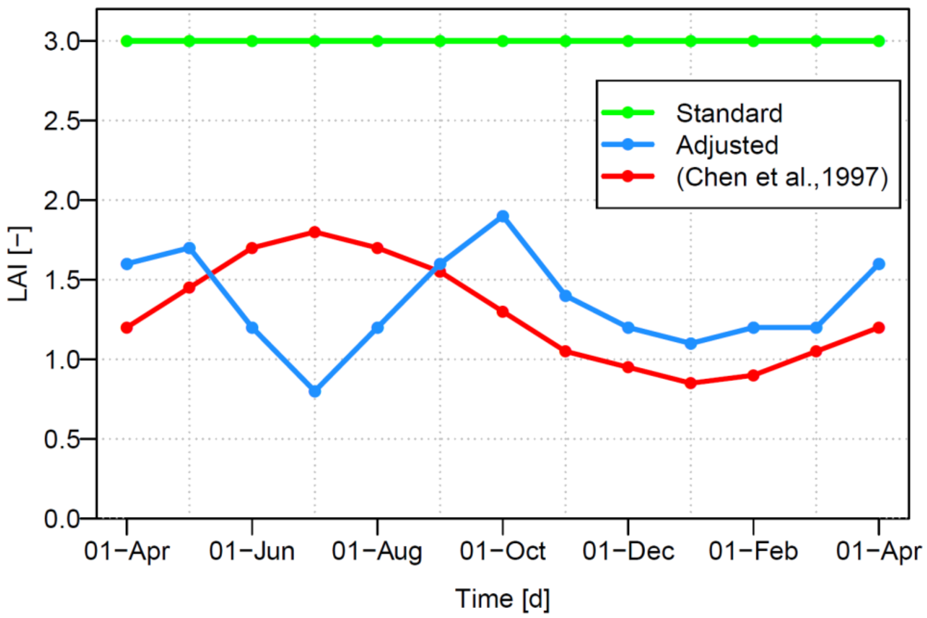

Figure 3.10 Montly LAI values (dots) and interpolated LAI by SWAP (lines).

performance. The LAI values with resulted in the highest Nash-Sutcliffe efficiency are used for further analyses and are named "LAI adjusted".

Based on the two parameters (K_{sat} and LAI) four scenarios were made to do a sensitivity analysis. The four scenarios made with varying LAI (see Figure 3.10) and K_{sat} values are as follows:

1. LAI adjusted, K_{sat}=23.41 cm d^{-1}
2. LAI adjusted, K_{sat}=9.65 cm d^{-1}
3. LAI (Chen et al., 1997), K_{sat}=23.41 cm d^{-1}
4. LAI constant, K_{sat}=23.41 cm d^{-1}

3.6 Overview

Table 3.6 Overview of hydrological models used in this study.

	HBV	Wag.	SAC-SMA	LGSI	SWAP
Input variables day	*P,T,ET,Q*	*P,ET,Q*	*P,ET,Q*	*P,ET,Q*	*P,ET,Q*
Input variables hour	*P,T,ET,Q*	*P,ET,Q*	*P,ET,Q*	*P,ET,Q*	*P*, Solar radiation, *T*, e_{rel}, v_{wind}, *Q*
Number of parameters	14	11	13	17	61
Calibration method	Genetic + local Powell	L-BFGS-B	L-BFGS-B	-	-
Version	2	2-2-2012	Hydromad 0.9-13	21-3-2012	3.2.36
Software	HBV-light graphical user interface	R code by Claudia Brauer	R-package from Hydromad project	R code by Ype van der Velde	Fortran
Reference	(Seibert, 1997)	(Stricker and Warmerdam, 1982)	(Burnash, 1995)	(Van der Velde et al., 2009)	(Van Dam, 2000)

4. Calibration, validation and simulation of whole years

4.1 Defining simulation periods

It is important that the models are calibrated correctly to have a valid comparison of the output. For each model it is tried to use the same time periods for calibration, validation and simulation (Table 4.1). HBV, Wageningen Model and SAC-SMA model use a one year warming up period before the calibration period. HBV and SAC-SMA simulate this warming up period separately to generate an initial value for the model parameters. The Wageningen Model has been given initial parameter values. The 4 year calibration period used for the daily data contains a variety of hydrological events so that the model is calibrated on different hydrological situations. SWAP and the Wageningen Model have also been run with hourly data. HBV, SAC-SMA and LGSI did not have the option of calibrating on hourly data in the specific codes used in this study. These hourly time series contained many gaps, which resulted in the choice to calibrate the models with an hourly time scale on discharge data between 1997 and 1999.

Table 4.1 Time periods in hydrological models

Period	Start	End
Calibration (day)	01-Apr-1991	01-Apr-1995
Calibration (hour)	01-Apr-1997	01-Apr-1999
Validation	01-Apr-2001	01-Apr-2003
Simulation	01-Apr-2010	01-Apr-2011

SWAP and LGSI were run for all three periods mentioned in Table 4.1, although they were not calibrated. Within SWAP a sensitivity analysis was performed for the parameters K_{sat} and LAI. This was done by defining four scenarios (see Section 3.5.2). LGSI had already been calibrated in a previous study by Van der Velde et al. (2009), the parameters from this study were used to run the model

To validate the parameter set a validation period is defined. The validation is needed because a good fit in the calibration period does not necessarily mean a correct set of parameters is found. Calibration may have been done purely by numerical fitting, resulting in parameters which do not conceptualize the hydrological system in the model structure correctly and are physically not reasonable. When for the validation period, with roughly a similar variety of hydrological events, a good fit is found, it can be considered that the calibrated model is valid for further use. For simulating the precipitation event a one year period from April 2010 to April 2011 is used.

4.2 Assessment of model performance: Nash-Sutcliffe efficiency

In hydrological studies the Nash-Sutcliffe efficiency (NSE or R^2) is one of the most often used assessment criteria (Krause et al., 2005). There exists however a large variety of assessment criteria in hydrology, as has been shown by lists made by Moriasi et al. (2007), Dawson et al. (2007) and Reusser et al. (2009). The Nash-Sutcliffe puts emphasis on the 20 % largest flows, while using the Nash-Sutcliffe on inverse discharge puts emphasis on the 20 % lowest flows (Pushpalatha et al., 2012). Because the interest in this study goes to simulating the discharge peaks, the Nash-Sutcliffe efficiency on normal discharge series has been used as measure for the performance of the models.

The Nash-Sutcliffe efficiency is defined as (Nash and Sutcliffe, 1970):

$$NSE = 1 - \frac{\sum(Q_{obs} - Q_{sim})^2}{\sum(Q_{obs} - \overline{Q_{obs}})^2} \qquad (1)$$

Where:

NSE	Nash-Sutcliffe coefficient	[-]
Q_{obs}	Observed discharge	[mm time^{-1}]
Q_{sim}	Simulated discharge	[mm time^{-1}]

The range of the Nash-Sutcliffe efficiency lies between $-\infty$ and 1. A perfect fitting model yields a value of 1. A value of zero indicates that the model is just as good in predicting the catchment response as the mean of all observed values. An efficiency higher than 0.70 is generally considered to be a good model result, but this also depends on the purpose of the model.

The Nash-Sutcliffe efficiency, or any other assessment criteria, can be used as an objective function for automatic calibration of models. This means that, with an optimization algorithm, the response surface of such an objective function can be searched for the parameter values that yield the best values of the objective function. The Nash-Sutcliffe efficiency is used as the objective function for the automatic calibration procedure in this study. Different optimization algorithms are implemented within the models to search for the optimal set of parameters.

When the hydrological models are calibrated and a simulation run is done the performance of the models is finally assessed by the following four criteria:

1) The value of the Nash-Sutcliffe efficiency
2) A visual inspection of the modelled and observed discharge around the highest discharge peak:
   - Start of rising limb
   - Time to peak
   - Value of discharge peak
   - The recession curve
3) A comparison of accumulated modelled and observed discharge over the whole simulation period and over a defined period from 14-August-2010 to 20-September-2010.
4) If applicable, the contribution of each flow route in the model.

4.3 Results of calibration, simulation and validation

All models were run four times for each period (calibration, validation, simulation). The Wageningen Model was given 4 different starting parameter sets, and HBV and SAC-SMA used a warming up period to generate a starting parameter set. LGSI used 4 given parameter sets. In SWAP four scenarios were defined, because SWAP supposedly does not need calibration as the parameters in SWAP are in principle observable. The range in Nash-Sutcliffe efficiency values is illustrated in Figure 4.1 with dots.

The first scenario of the Wageningen Model with hourly time resolution and constant parameters resulted in very poor results. It can thus not be assumed that daily process parameters in a model can directly be converted to hourly values. The results of this model run will therefore not be mentioned further in this study. Every model, except SWAP, performed well for each period and had Nash-Sutcliffe values of at least 0.6 for each run (Figure 4.1). The highest average efficiency is reached for the calibration period, with exception of SWAP. Because the adjustments in SWAP were done in such a way to obtain a good fit for the simulation period, only the first scenario resulted in a good fit for the simulation period. The effect of the adjustment in LAI depends very much on how wet a year is. During dry periods a lower LAI will not reduce evapotranspiration as much as during wet periods. Therefore the efficiency of SWAP varies very strongly between the model periods. The validity of the model for different time periods or a different time discretization is highly unstable. The range in efficiency for the simulation period for the Wageningen Model is small compared to the other models. Also during the validation period the range is not very large. The four parameter sets found with the Wageningen Model are almost equally good in simulating discharge during different periods with more extreme values, while the validity of each parameter set in the other models does depend on the variety of hydrological events during a year.

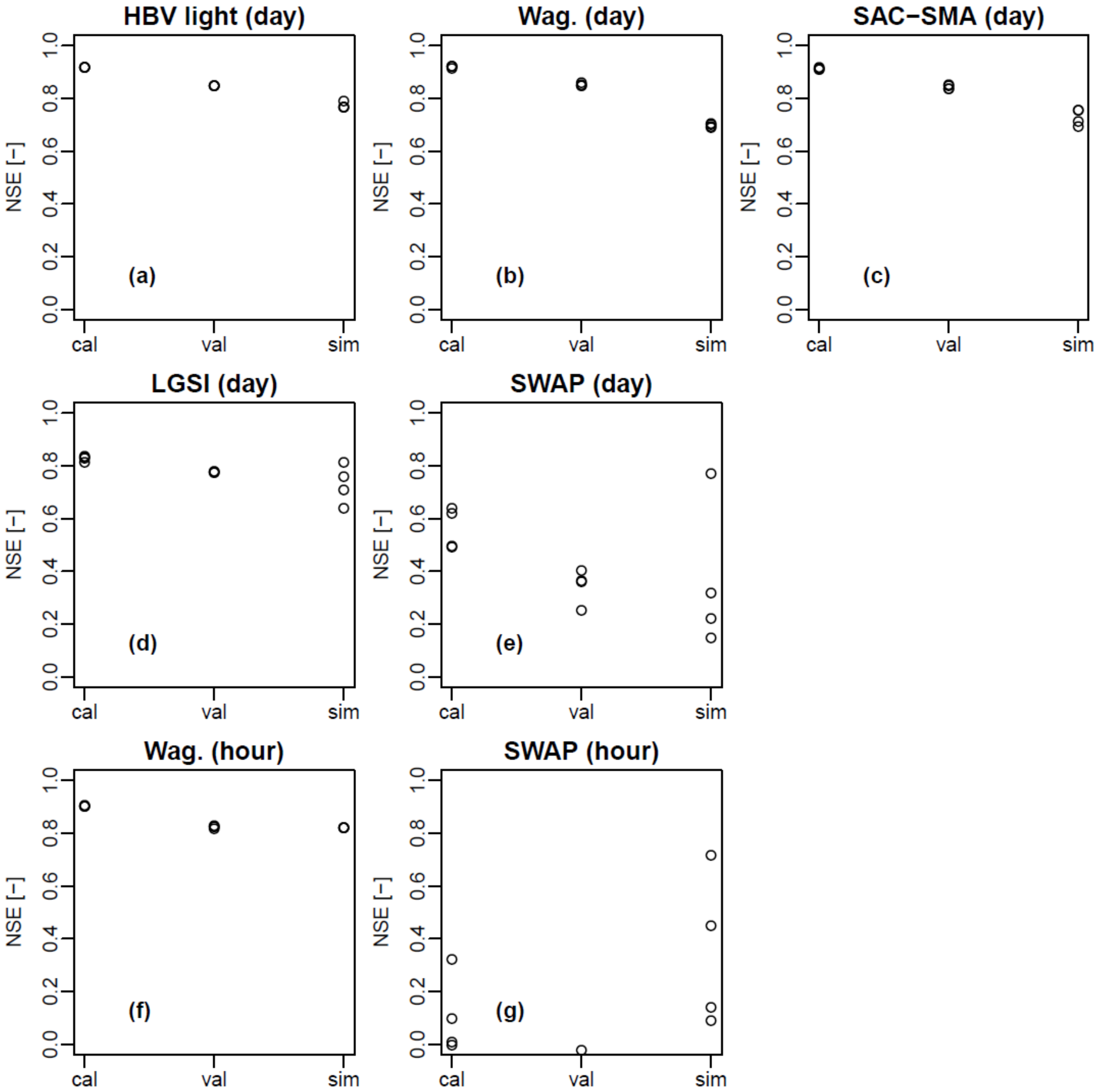

Figure 4.1 Range in Nash-Sutcliffe efficiency (NSE) values for four model runs. (a)-(e) Model runs with daily data. (f)-(g) Model runs with hourly data. The abbreviation cal stands for the calibration period, val for the validation period, sim for the simulation period.

The parameter set which resulted in the best fit for the calibration and validation period was chosen for further analyses. For SWAP the first scenario was chosen. The complete 4 sets of parameters for HBV, Wageningen Model and SAC-SMA are given in Appendix A, the parameter sets used in LGSI in section 3.4.2, and for SWAP in Appendix B. The set with an underscore was the best run, and the results of this run are given in Table 4.2. For the daily data LGSI has the highest efficiency during the simulation period and simulated the observed discharge peak of 42.2 mm/d best (35.9 mm/d). The Wageningen Model resulted in the best fit for the hourly data and simulated the observed peak discharge of 2.8 mm/h very closely (2.9 mm/h).

Table 4.2 Nash-Sutcliffe efficiencies for the best run for the calibration, validation and simulation period. For the simulation period the simulated peak discharge is given.

Model	Calibration	Validation	Simulation	
	NSE	NSE	NSE	*Q* peak
HBV	0.917	0.848	0.766	28.3 mm d^{-1}
Wag (day)	0.912	0.860	0.703	27.7 mm d^{-1}
SAC-SMA	0.913	0.851	0.756	22.6 mm d^{-1}
LGSI	0.833	0.778	0.811	35.9 mm d^{-1}
SWAP (day)	0.619	0.403	0.769	26.5 mm d^{-1}
Wag (hour)	0.904	0.828	0.821	2.9 mm h^{-1}
SWAP (hour)	0.008	-0.078	0.717	3.1 mm h^{-1}

From the sum and change of different variables in each model during the simulation period the water balance has been calculated (Table 4.3). No further data could be obtained from SAC-SMA than simulated discharge. The calculated balance for this model only gives the amount of water which is either evaporated or stored. For SWAP and LGSI the change of total storage throughout the profile has been calculated, thus groundwater level change does not change the water balance. None of the water balances closes completely. The Wageningen Model (day), SWAP (day) and LGSI have an almost closing water balance, but HBV, Wageningen Model (hour) and SWAP (hour) differ from -5.2 mm to 16.2 mm. The imbalance in HBV of 16.2 mm is quite substantial (1.9 % of total influx). Small imbalances (i.e. <0.5 mm) may actually be caused by rounding errors in the models itself. None of the simulated discharge in the models exactly agrees to what was observed (*Q* obs = 474.3 mm). For SWAP the first scenario was chosen as best run. The LAI was adjusted in this scenario to reduce the evapotranspiration values, so that groundwater levels do not fall to deep. The simulated actual evapotranspiration is in line with the simulated evapotranspiration values by the other models. Graphs of the variation of all variables for each model during the simulation period is given in Appendix C.

Table 4.3 The sum and change of different variables in each model, and a water balance for the simulation period.

Time discr.	Model	P [mm]	Q sim [mm]	ET_{act} [mm]	ΔSM [mm]	ΔSLZ [mm]	ΔSUZ [mm]	ΔSTZ [mm]	Balance [mm]
Day	HBV	867.4	437.3	438.4	-18.8	-5.7	0.0	0.0	16.2
Time discr.	**Model**	**P [mm]**	**Q sim [mm]**	**ET_{act} [mm]**	**ΔSM [mm]**	**ΔGstore [mm]**	**ΔSlow box [mm]**	**ΔFast box [mm]**	**Balance [mm]**
Day	Wag.	867.4	498.2	417.7	-15.3	-15.2	-0.3	-33.1	0.2
Hour	Wag.	867.4	531.6	403.2	-42.6	-22.7	0.0	-19.6	-5.2
Time discr.	**Model**	**P [mm]**	**Q sim [mm]**	**ET_{act} [mm]**	**ΔStorage [mm]**	**ΔGWL [cm]**	**-**	**-**	**Balance [mm]**
Day	SWAP	867.4	402.5	436.4	28.4	31.2	-	-	0.1
Hour	SWAP	867.4	401.5	431.5	30.0	34.0	-	-	4.3
Day	LGSI	867.4	436.7	384.4	46.1	23.2	-	-	0.2
Day	SAC-SMA	867.4	455.2	-	-	-	-	-	412.2

4.4 Sensitivity analysis with SWAP

To analyse the influence of the adjustments in LAI and K_{sat} four scenarios were made for the SWAP model:

1. LAI adjusted, K_{sat} = 23.41 cm d^{-1} (Figure 4.2a and b)
2. LAI adjusted, K_{sat} = 9.65 cm d^{-1} (Figure 4.2c and d)
3. LAI (Chen et al., 1997), K_{sat} = 23.41 cm d^{-1} (Figure 4.2e and f)
4. LAI = 3 (constant), K_{sat} = 23.41 cm d^{-1} (Figure 4.2g and h)

When the LAI is set to 3 and K_{sat} to 23.41 cm d^{-1} SWAP will almost give no response to the precipitation event (Figure 4.2g). Due to high evapotranspiration values the groundwater will drop very deep. All precipitation will then be used to refill the soil with moisture.

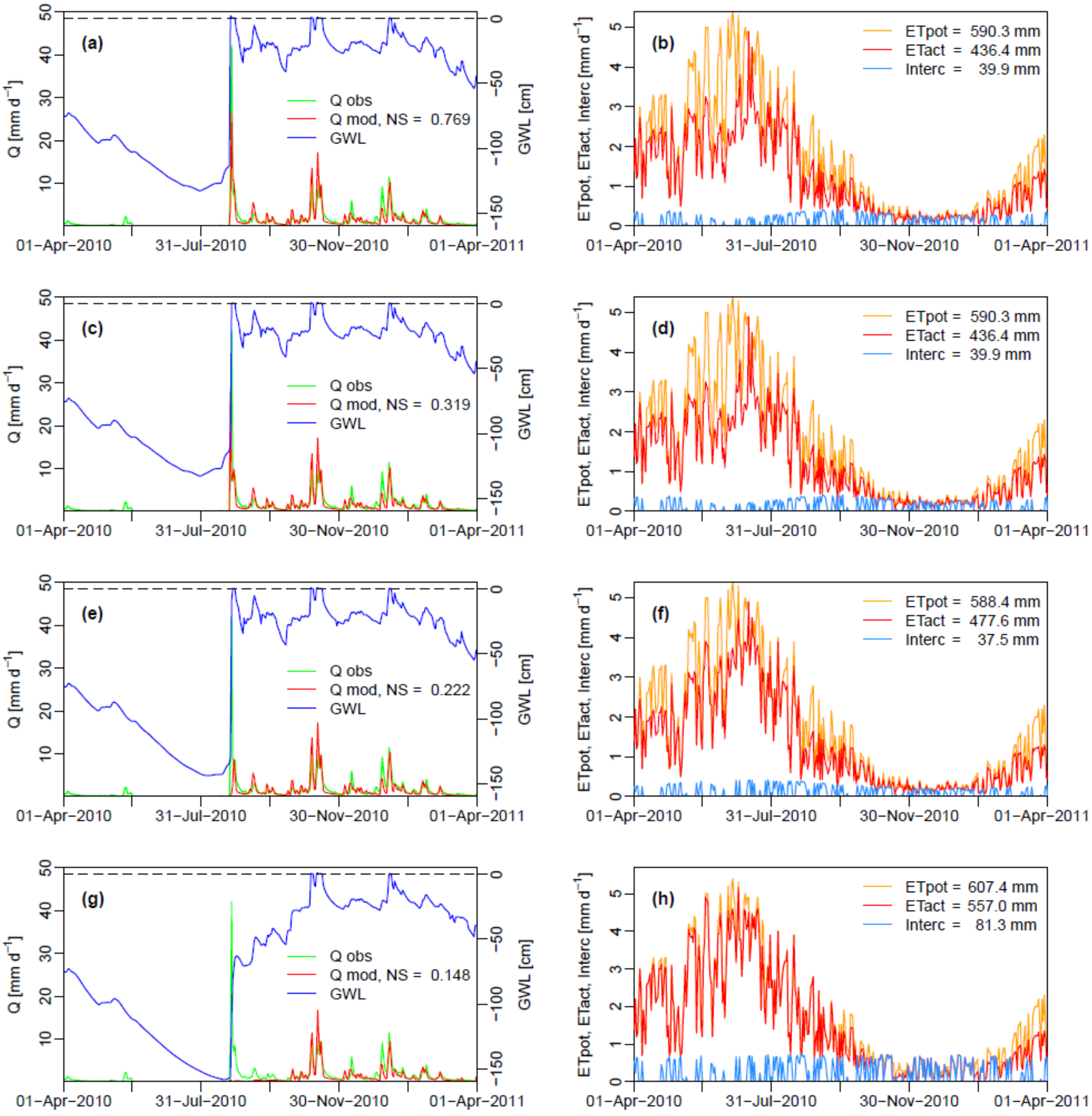

Figure 4.2 Simulated discharge, GWL and ET changes due to varying LAI and K_{sat} value. (a)-(b) Scenario 1, (c)-(d) Scenario 2, (e)-(f) Scenario 3 and (g)-(h) Scenario 4. The dashed line represents land surface.

Using the monthly variation in LAI as proposed by Chen et al. (1997) the discharge does give a small response and groundwater levels rise much faster after the precipitation event. Still the evapotranspiration values are rather high (477.6 mm) compared to the other models and the efficiency low (0.222). The adjusted monthly variation in LAI given in Figure 4.2a through 4.2d results in a more realistic response of discharge. However the Nash-Sutcliffe efficiency is very poor (0.319) when the K_{sat} value is used according to Wösten et al. (1994). The main reason the model has this low efficiency is due to timing of the discharge peak and the time it takes the water is discharged. In Figure 4.2c can be seen that the discharge rises very quickly to peak before the measured discharge peak. After the discharge peak the simulated discharge very quickly falls down. This timing results in a very large squared errors, and hence in a very small efficiency. The reason for the quick response is that the water is mainly runoff water and less discharge from the subsoil. Increasing the saturated hydraulic conductivity to 23.41 cm d^{-1} will result in more infiltration and therefore less runoff. In Figure 4.3a can be seen that the timing of the discharge peak is much better and with that the efficiency of the model. Exactly the same response pattern was observed for the hourly data.

Figure 4.3 shows that decreasing the LAI will in general result in lower transpiration and interception values, but higher evaporation values. Evaporation becomes higher because more water falls through on the land surface (less interception) and the top soil gets wetter due to less water uptake by plants. The same

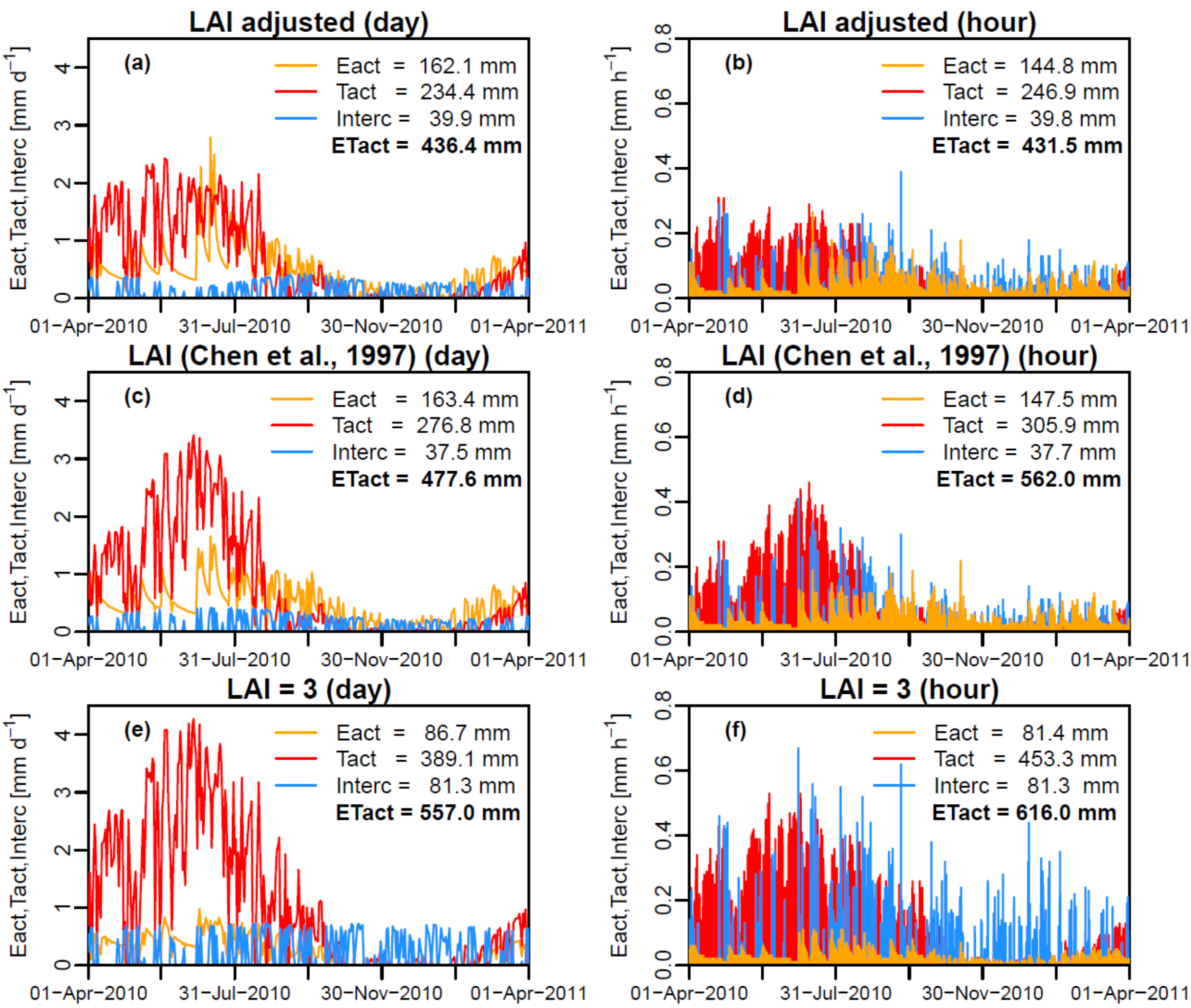

Figure 4.3 Actual evaporation, transpiration and interception change due to variation in LAI as modelled by the SWAP model. (a) and (b) LAI adjusted, daily and hourly values respectively, (c)-(d) LAI (Chen et al., 1997) daily and hourly values respectively; (e)-(f) LAI = 3 daily and hourly values respectively.

pattern can be observed for the hourly data. The calculated sum of evaporation does not increase and interception decrease with lowered LAI (compare Figure 4.3c and 4.3d with 4.3a and 4.3b). This is because the adjusted monthly LAI values were set higher for some months compared to the values found by Chen et al. (1997) (see Figure 3.10), making the balance of interception and evaporation for the whole year comparable.

The increase of soil evaporation values with decreasing LAI could explain the reason for the low Nash-Sutcliffe efficiency for the SWAP model with the second scenario (Figure 4.2c). The difference in groundwater level and evapotranspiration between the first and seconds scenario is very small. Therefore the expectation would be that the simulated discharge would agree better between the scenarios. Decreasing the LAI will however result in wetter top soils and therefore more runoff, compared to the original constant LAI value. Because less water is abstracted by plants for transpiration groundwater levels will not fall down as much anymore, and the discharge response will consist more and more of a fast component. This causes the discharge around the peak to rise very quickly, but also to decline more quickly than in the first scenario. This results in poor model performance since the Nash-Sutcliffe values is calculated with squared differences. For the first scenario the saturated hydraulic conductivity is however increased. Increasing the saturated hydraulic conductivity of the top soil will result in more infiltration and a reduction of increased runoff. This results in better model performance.

5. Simulation of the flood event

5.1 Discharge

In this paragraph the model simulations during the event period from 14 August 2010 to 20 September 2010 are analysed. Figure 5.1 and Figure 5.2 show the simulated discharge for the daily and hourly time step respectively. The rising limb of the observed discharge peak starts on 25 August (day) and on 26 August 07:00 UTC (hour). In Figure 5.1a and 5.2a the initial discharge at this time is given.

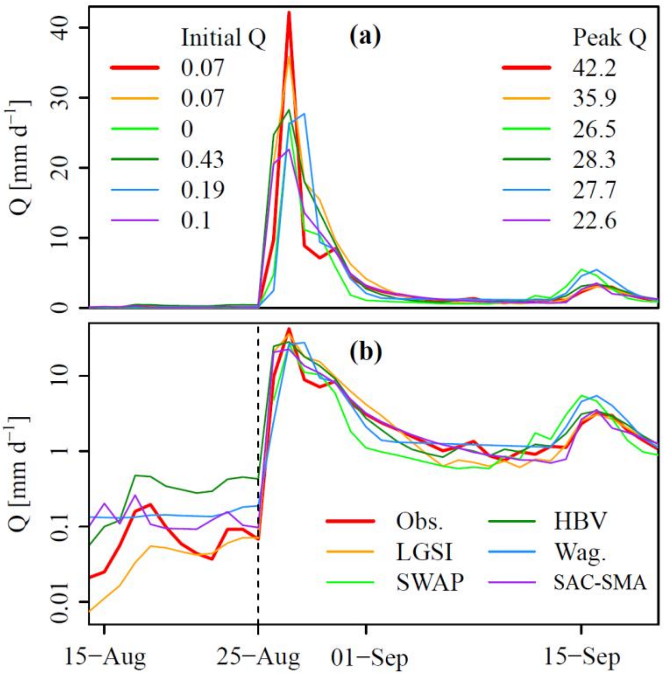

Figure 5.1 Simulated discharge for daily data on linear axis (a) and logarithmic axis (b).

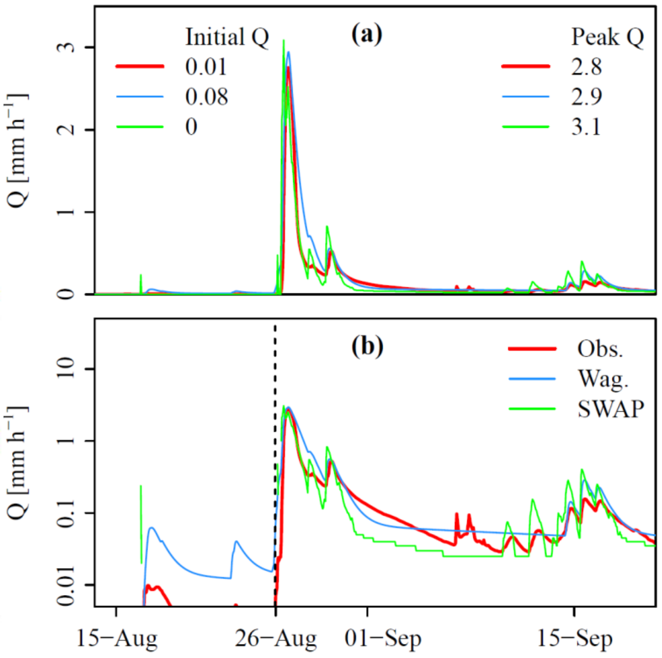

Figure 5.2 Simulated discharge for hourly data on linear axis (a) and logarithmic axis (b).

For the daily data the models fit the observed data quite well, although peaks are underestimated. LGSI begins with exactly the same initial discharge as observed and describes the peak quite well; for the models with daily data it has the highest Nash-Sutcliffe efficiency (Table 5.1). Other models show a more flattened peak. The rising limb of the SAC-SMA model, HBV and LGSI are in the beginning steeper than observed. SWAP and the Wageningen Model have a less steep rising limb and also have a higher Lag 1 of 3 days (Table 5.1). The definition of RR, Lag 1 and Lag 2 is explained in Section 2.4. The Wageningen Model simulates the discharge

Table 5.1 Analysis of the discharge hydrograph. NS efficiency, runoff ratio (RR), lag time and date of start and peak of rising limb for the period 14-08-2010 to 20-09-2010.

Time discr.	Model	NS [-]	RR [-]	Lag 1 [d]	Lag 2 [d]	Start rising limb	Date *Q* peak
	Obs.	-	0.38	2	1	25-Aug-2010	27-Aug-2010
	HBV	0.699	0.45	2	1	25-Aug-2010	27-Aug-2010
Day	Wag.	0.623	0.40	3	2	25-Aug-2010	28-Aug-2010
	SAC-SMA	0.704	0.38	2	1	25-Aug-2010	27-Aug-2010
	LGSI	0.823	0.46	2	1	25-Aug-2010	27-Aug-2010
	SWAP	0.820	0.31	3	1	25-Aug-2010	27-Aug-2010
Time discr.	**Model**	**NS [-]**	**RR [-]**	**Lag 1 [h]**	**Lag 2 [h]**	**Start rising limb [UTC]**	**Date *Q* peak [UTC]**
	Obs.	-	0.38	42	10	26-Aug-2010 07:00	27-Aug-2010 03:00
Hour	Wag.	0.858	0.51	33	11	26-Aug-2010 05:00	27-Aug-2010 04:00
	SWAP	0.748	0.38	32	3	26-Aug-2010 09:00	26-Aug-2010 20:00

peak one day later than the observed discharge peak on 27 August. During the falling limb the SAC-SMA model is closest to the observed discharge. The SAC-SMA has also the same runoff ratio (RR) as observed.

For the models with hourly time resolution the Wageningen Model had a high Nash-Sutcliffe efficiency (0.858). The start of the rising limb is however two hours earlier than observed, and for the SWAP model two hours later than observed. The Lag 1 for the Wageningen Model is 9 hours shorter than observed, and for SWAP 10 hours shorter. This is remarkable because in case of a daily time resolution both models had a lag time one day longer than observed. The discharge peak of the Wageningen Model is one hour later and for SWAP 7 hours earlier, which can also be seen by looking at the Lag 2. The reaction time (time to peak) is thus very short, which could be caused by the wet top soils due to lower LAI (see Section 4.4). The SWAP model did simulate almost no discharge until 26 August.

5.2 Soil moisture and groundwater

The wetness of the catchment before the event is very important to be incorporated correctly in a hydrological model as has been shown by for example Noto et al. (2008) and Brauer et al. (2011). Low initial soil moisture conditions dampen the discharge response of the catchment to precipitation events. Therefore it is interesting to look at the response of soil moisture and the groundwater level to the observed precipitation as was modelled by the different models. Only from SAC-SMA no soil moisture or groundwater level data were available.

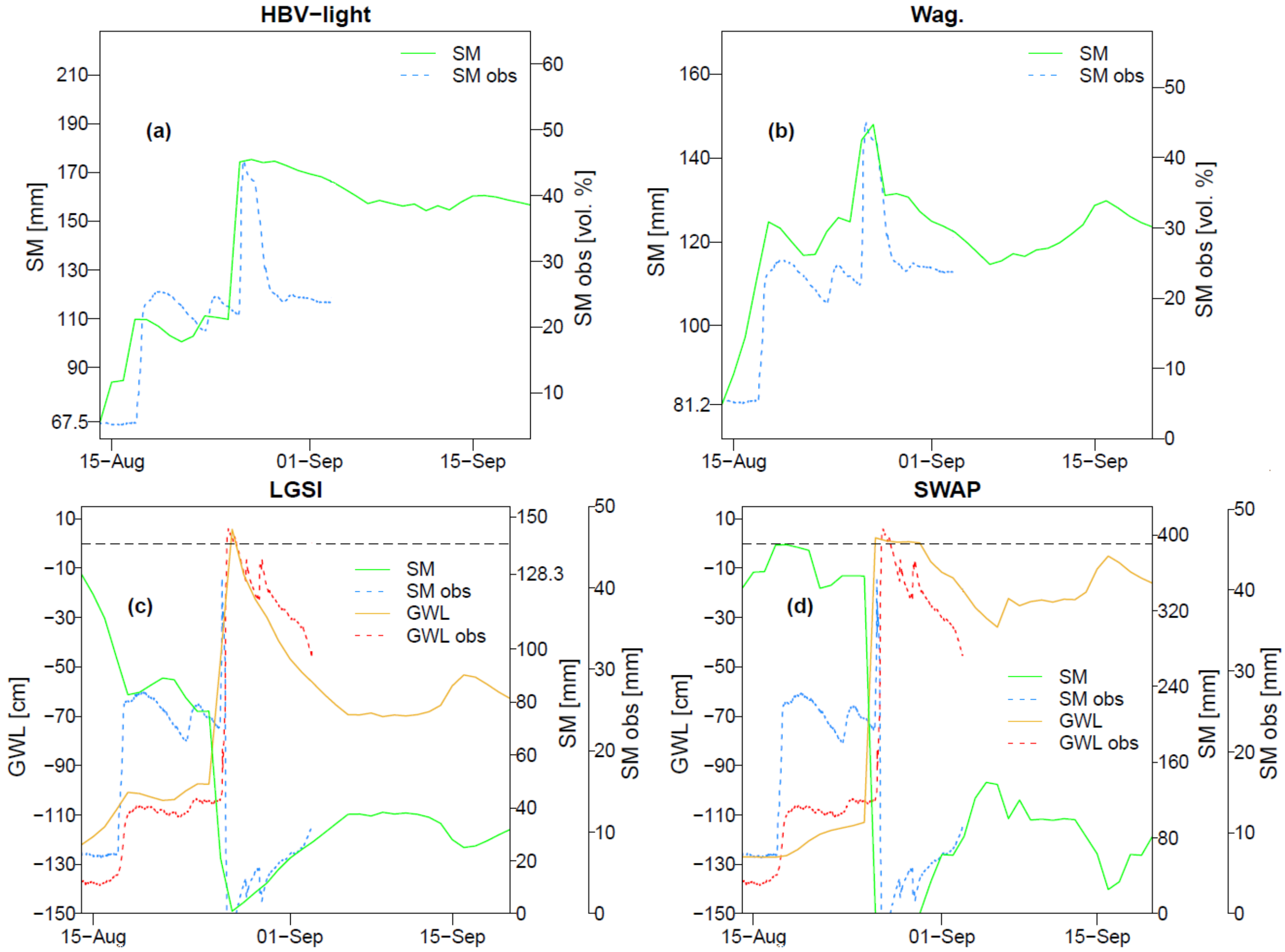

Figure 5.3 Response of soil moisture and (if available) groundwater level to precipitation input signal for the models with a daily time step. The dashed black line in (c) and (d) represents land surface.

The amount of soil moisture given by HBV and the Wageningen Model is the amount of water stored above a groundwater zone with a fixed level. SWAP gives the soil water content (cm^3 cm^{-3}) at 34 depths in the soil profile. Multiplying the soil water content with the thickness of each accompanying soil compartment for the soil column above the groundwater level, and adding these values up, will give the amount of water stored in the unsaturated for the SWAP model. LGSI gives, a bit non-intuatively named, the air-filled pore volume in the unsaturated zone (named storage unsaturated zone) and the total pore volume in the unsaturated zone (named storage saturated zone). For LGSI the difference between the total pore volume and air-filled pore volume in the unsaturated zone zone gives the storage in the unsaturated zone. In Figure 5.3 and 5.4 the amount of water in the unsaturated zone has been plotted for the models. Two assumptions were made in Section 2.4 about soil moisture levels: the observed storage in the unsaturated zone equals the soil moisture content at 40 cm depth times the groundwater depth, and the shape of the response curve of soil moisture content equals the shape of simulated soil moisture stored in a reservoir. With these assumptions the shape of the simulated soil moisture in HBV and Wageningen Model should resemble the shape of the observed soil moisture content at 40 cm depth. The simulated soil moisture in SWAP and LGSI should then be equal to the observed storage in the unsaturated zone.

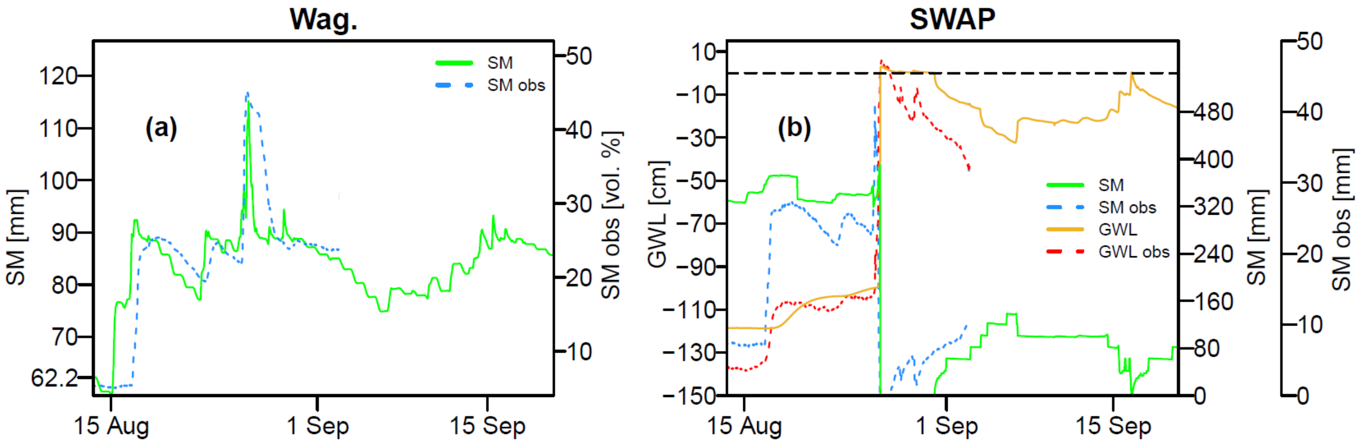

Figure 5.4 Response of soil moisture and (if available) groundwater level to precipitation input signal for the models with a hourly time step. The dashed black line represents land surface.

In Figure 5.3 can be seen that the shape of observed soil moisture content does not completely resemble the shape of the soil moisture in HBV and the Wageningen Model. Timing of the start of rising limbs or peaks is best simulated by the Wageningen Model, but they are not exactly the same. Also for LGSI and SWAP the amount of soil moisture is not the same as observed (notice the difference in axis). The amount of soil moisture is in the beginning of the event period much higher than observed. The soil moisture storage in the SWAP model is much larger than in the other models. Simulated and observed groundwater levels have the same order of magnitude. Observed groundwater levels were above surface from 21:15 at 26 August to 17:00 UTC at 27 August. The duration of ponding is better simulated in LGSI (1 day) than SWAP. SWAP simulates a too long period of ponding for the daily (5 days) and hourly time resolution (4 days and 13 hours) (Figure 5.3 and Figure 5.4). Because water does not infiltrate due to a saturated soil profile, water stays on the soil surface. This water could stay too long on the soil surface before it can run off, due to a too high overland resistance (γ) or an incorrect parameter value for the critical ponding layer depth ($h_{0,threshold}$). Increasing the LAI resulted in more transpiration, and lower groundwater levels, but a good fitting model could then not be found. For the Wageningen Model with hourly resolution soil moisture started to rise significantly at 15:00 UTC on 26 August, 8 hours later than observed. For SWAP a small increase in soil moisture was observed at 9:00 UTC, but at 23:00 UTC groundwater reached surface reducing soil moisture storage to zero. Groundwater remained above surface until 12:00 UTC on 31 August. It has to be noted that groundwater levels were measured at only two locations in one field. Locally water levels could have responded much differently than in this specific field. Assuming groundwater levels in this field to be representative for the whole catchment could be incorrect. Therefore it can be possible SWAP actually represents the catchment average groundwater level better than

LGSI. Only with many piezometers dispersed throughout the catchment a reliable comparison can be made to what is simulated. This spatial variation also applies to the soil moisture content.

The total fluxes simulated by the models from the start of the simulation period to the discharge event are given in Table 6.4. During this period 28.8 mm of discharge was observed and 434.5 mm of potential evapotranspiration. LGSI and SWAP simulate very little discharge until 25 August. SWAP even simulates completely no discharge between 15 April and 25 August. For most models soil moisture declines from 1 April to 25 August, which shows that before the event period the catchment had dried up to some extent.

Table 5.2 Hydrological pre-event water balance. Total discharge, ET act, and initial and final SM for the period 01-04-2010 to 25-08-2010.

Time discr.	Model	$\Sigma Q\ sim$ [mm]	ΣET_{act} [mm]	*SM* 1 Apr [mm]	*SM* 25 Aug [mm]
Day	HBV	29.2	288.2	157.8	109.7
	Wag.	56.3	261.0	123.5	124.8
	SAC-SMA	38.8	-	-	-
	LGSI	1.5	232.8	327.1	300.3
	SWAP	1.0	322.5	721.6	660.5
Hour	Wag.	67.2	249.0	113.6	87.8
	SWAP	2.3	289.5	720.5	682.5

5.3 Water balance

A water balance for the event period (14 Aug-20 Sep) is given in Table 5.3. SAC-SMA simulates the total amount of discharge best (Q obs = 114.2 mm), just as it did for the whole simulation period. The Wageningen Model with hourly data has as only model a completely closing balance, but simulated discharge is too high. HBV, SWAP and the Wageningen Model with daily data have an almost closing balance. Because groundwater levels remain much longer close to the land surface, for SWAP, the change in groundwater level is much larger compared to LGSI.

Table 5.3 The sum and change of different variables in each model and a water balance, calculated over a period from 14-08-2010 to 20-09-2010.

Time discr.	Model	P [mm]	Q sim [mm]	ET_{act} [mm]	ΔSM [mm]	ΔSLZ [mm]	ΔSUZ [mm]	ΔSTZ [mm]	Balance [mm]
Day	HBV	297.9	134.9	66.0	89.1	9.9	0.0	0.0	-2.0
Time discr.	**Model**	**P [mm]**	**Q sim [mm]**	**ET_{act} [mm]**	**ΔSM [mm]**	**ΔGstore [mm]**	**ΔSlow box [mm]**	**ΔFast box [mm]**	**Balance [mm]**
Day	Wag.	297.9	118.4	66.3	42.3	73.2	72.7	0.0	-1.8
Hour	Wag.	297.9	152.5	65.9	23.5	56.0	56.0	0.0	0.0
Time discr.	**Model**	**P [mm]**	**Q sim [mm]**	**ET_{act} [mm]**	**ΔStorage [mm]**	**ΔGWL [cm]**	**-**	**-**	**Balance [mm]**
Day	SWAP	297.9	91.4	47.9	160.7	110.9	-	-	-2.1
Hour	SWAP	297.9	111.7	48.5	137.0	102.3	-	-	0.7
Day	LGSI	297.9	137.8	60.9	130.5	59.2	-	-	-31.4
Day	SAC-SMA	297.9	113.7	-	-	-	-	-	184.2

5.4 Flow route contributions

In Figure 5.5 and Figure 5.6 each flow route contribution to the total discharge is given. These discharge components are given as a fraction of the total discharge. LGSI simulates almost all discharge coming from tube

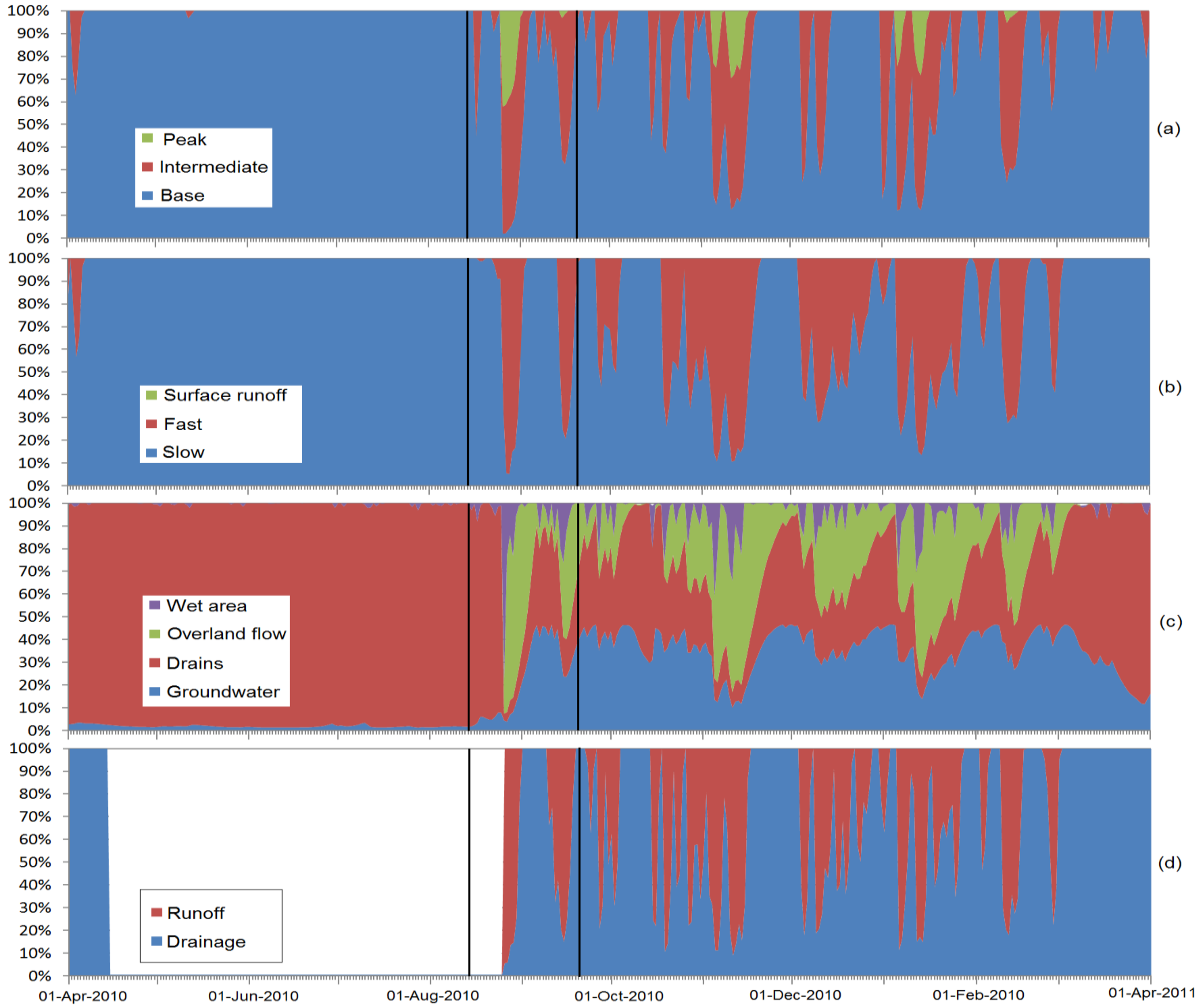

Figure 5.5 Discharge components as fraction of total discharge, as simulated by models with daily time resolution. Vertical black lines indicate the beginning and end of the event period. (a) HBV, (b) Wageningen Model, (c) LGSI and (d) SWAP.

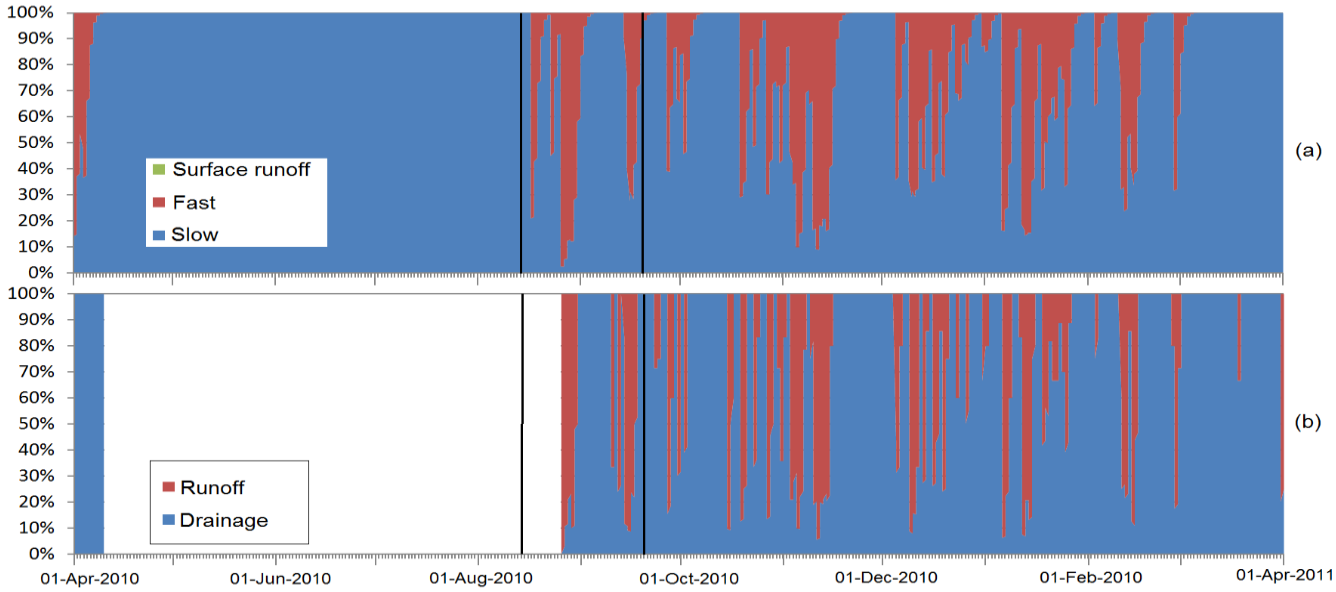

Figure 5.6 Discharge components as fraction of total discharge, as simulated by models with hourly time resolution. Vertical black lines indicate the beginning and end of the event period. (a) Wageningen Model and (b) SWAP.

drains until 26 August. Directly after the precipitation event most discharge originates from overland flow and from inundated areas. Not until after the precipitation event groundwater becomes a dominant contributor to total discharge, while in HBV and the Wageningen Model base flow is the main component already before the precipitation event. The contribution of tube drain flow for the period from November through May was averaged 22.1 %. Van der Velde et al. (2010) found for the same period in 2007-2008 a contribution of tube drain flow of 59 %. The slowest component in the discharge is for HBV base flow, in the Wageningen Model Slow flow, in LGSI groundwater flow and in SWAP drainage. The contribution of this slowest flow route for the simulation period is for these models respectively 44.47 %, 49.71 %, 22.88 % and 37.85 % for the daily time resolution (Table 5.4). For the hourly time resolution the Wageningen Model has 48.0 % and SWAP has 36.49 % as slowest contribution. Only HBV gives the slow flow route as major contributor to the total outflow for the simulation period. On average the slow flow route would be the largest contributor to the total outflow for a hydrological year.

Table 5.4 Total contribution of each flow route for the simulation and event period.

HBV	Simulation period			Event period		
Peak flow	61.34	mm	(14.03 %)	37.70	mm	(27.94 %)
Intermediate flow	181.47	mm	(41.50 %)	69.60	mm	(51.57 %)
Base flow	194.49	mm	(44.47 %)	27.65	mm	(20.49 %)
Wag (day)						
Surface runoff	0.00	mm	(0.00 %)	0.00	mm	(0.00 %)
Fast	250.53	mm	(50.29 %)	84.88	mm	(71.69 %)
Slow	247.67	mm	(49.71 %)	33.51	mm	(28.31 %)
LGSI						
Wet area	60.08	mm	(13.68 %)	33.69	mm	(23.79 %)
Overland	193.40	mm	(44.02 %)	76.18	mm	(70.57 %)
Drains	85.32	mm	(19.42 %)	14.45	mm	(14.53 %)
Groundwater	100.52	mm	(22.88 %)	17.32	mm	(15.93 %)
SWAP (day)						
Runoff	250.14	mm	(62.15 %)	67.68	mm	(74.04 %)
Drainage	152.35	mm	(37.85 %)	23.74	mm	(25.96 %)
Wag (hour)						
Surface runoff	0.00	mm	(0.00 %)	0.00	mm	(0.00 %)
Fast	276.41	mm	(52.00 %)	114.70	mm	(75.26 %)
Slow	255.17	mm	(48.00 %)	37.71	mm	(24.74 %)
SWAP (hour)						
Runoff	255.01	mm	(63.51 %)	88.19	mm	(78.94 %)
Drainage	146.52	mm	(36.49 %)	23.53	mm	(21.06 %)

For the event period an increase in the contribution of fast flow routes is simulated. The Wageningen Model, however, does not simulate surface runoff for this very wet period. In Appendix C can be seen the soil moisture in the Wageningen Model never reaches saturation, and therefore the model never produces surface runoff. Because observed soil moisture reaches saturation and groundwater levels reach land surface (Figure 2.3) after the precipitation event, it can be concluded that the Wageningen Model does not simulate this part correctly. A possible explanation is that the new soil moisture content is calculated with too many iteration steps. In every step the new soil moisture is calculated by adding the precipitation to, and subtracting the evapotranspiration and percolation from, the old soil moisture content. Percolation is calculated based on the new soil moisture content. When the soil moisture content is very high, percolation will be very high, causing the soil moisture calculated in the next iteration step to be low and to stay low. Other factors could cause the low soil moisture contents as well, but too many iterations steps is definitely the most important one.

SWAP makes a mistake by not simulating any discharge between 15 April and 25 August. Even in drier periods there is always some discharge.

6. Discussion

6.1 Choice of algorithm

The choice of the algorithm to search the response surface of the objective function may influence the final set of parameters the model will find. Some algorithms have a global search strategy, finding a global maximum, others have a local search strategy, possibly missing out a higher peak further away. HBV searches the user defined objective functions with a combination of a global genetic algorithm and a local optimization algorithm. The Wageningen Model and SAC-SMA use a limited-memory Broyden-Fletcher-Goldfarb-Shanno quasi-Newton optimization algorithm with bounds on the variables (L-BFGS-B). This algorithm is often used to solve large nonlinear optimization problems. Seibert (2000) discusses the results from Franchini et al. (1998) who only found slight differences in performance between a genetic algorithm with a local optimization as used in HBV and a Shuffled Complex Evolution algorithm (SCE-UA). This SCE-UA is a global optimization algorithm, which combines the strengths of a simplex procedure of (Nelder and Mead, 1965) with the concepts of controlled random search, genetic evolution and the concept of shuffling.

Hydromad not only offers the possibility to easily compare the different implemented hydrological models, but also to compare different optimization algorithms. In total 10 algorithms are available in Hydromad, including SCE-UA and L-BFGS-B. When, based on the findings of Franchini et al. (1998), the assumption is made that the performance of the algorithms within HBV are similar to the SCE-UA algorithm, hydromad can offer the opportunity to have insight in the relative influence of a chosen algorithm on the performance of the hydrological model. Figure 6.1 gives the optimization traces of 9 algorithms for the SAC-SMA model. The Dream algorithm is not taken into account, because it gave the least good results and had a very slow convergence. The 9 algorithms were run with the same initial set of random parameters and a total of 100 samples. Only L-BFGS-B and DE were given different settings, respectively 15 samples and a maximum of 1300 iterations. This because the efficiency did not increase when more samples were used in case of the L-BFGS-B algorithm and because more iterations significantly increased the number of function evaluations without increasing the efficiency in case of the DE algorithm. In Figure 6.1 the order in performance in terms of the Nash-Sutcliffe efficiency can be seen. The DE (NS=0.919), PORT (NS=0.919), L-BFGS-B (NS=0.915), SCE-UA (NS=0.909) and Nelder-Mead (NS=0.907) are the top five performing algorithms. From these five, the SCE-UA and L-BFGS-B have the fastest convergence making them the preferable choice for the SAC-SMA model. Some

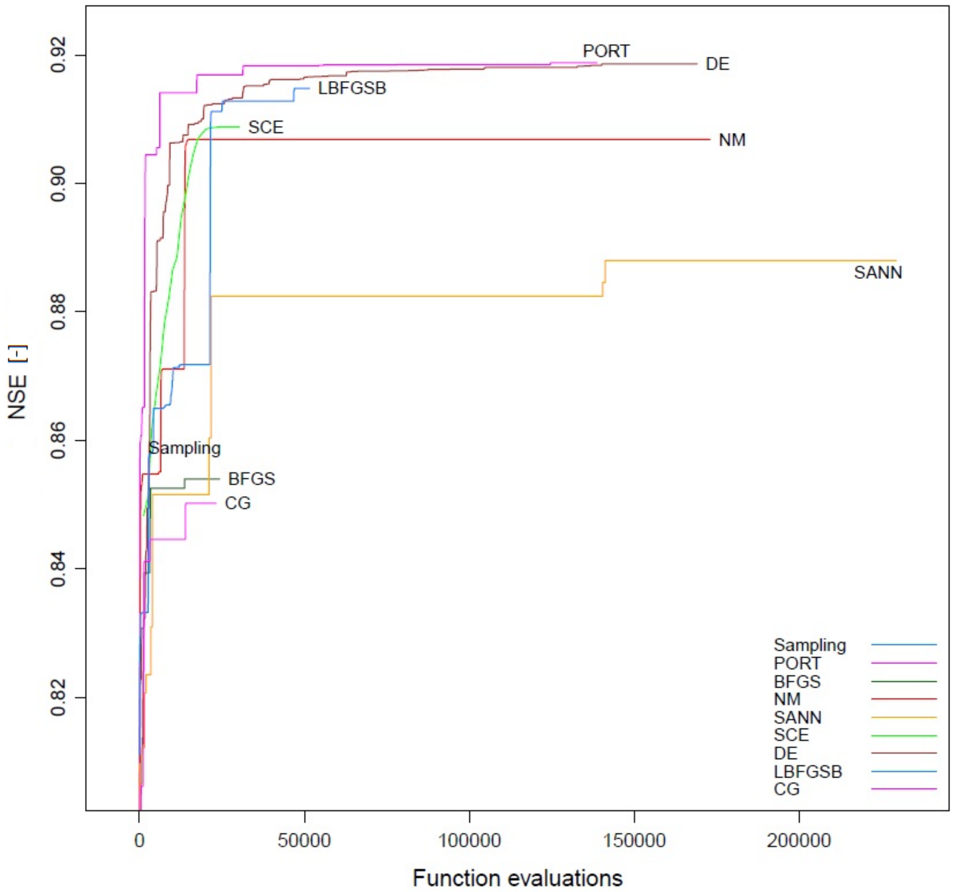

Figure 6.1 Optimisation traces from 9 algorithms in calibrating the SAC-SMA model using an R^2 objective function.

algorithms like Nelder-Mead and PORT are in general most appropriate in simulation studies with large models (Andrews et al., 2011). Considering that the maximum number of parameters is 14 for the HBV model, only one more than the SAC-SMA model, an increase in performance from these two algorithms is not expected. With only a difference in efficiency of 0.006 between SCE-UA and L-BFGS-B it may be assumed the performance of the different hydrological models used in this thesis will not be significantly influenced by the choice of algorithm.

6.2 The goodness of fit

Best model efficiencies for the daily time steps were found for the LGSI model (NS=0.811). For the hourly data the Wageningen Model fitted the measured data well (NS=0.821). Using a higher time discretization in general improves model results for short flashy phenomena in catchments. When flooding is at stake timing of discharge peaks is of uttermost importance. Using hourly time steps will help in simulating the exact timing of these peaks. However, when only long term fluxes and model efficiencies in general are important models using daily time steps can perform just as good as models with hourly data. The specific questions to which the hydrological models must give an answer largely determine what time discretization is most appropriate. The reason that a higher time discretization is in general better, is because most lumped models use threshold values in their model structure. Outflow of certain reservoirs will only take place at a certain storage or flow rate. By using daily input data most of the extreme peaks during a day are averaged out, which might result in no outflow of certain reservoirs and an underestimation of discharge peaks. The results obtained with LGSI show that modelling on a daily time scale can however give an accurate timing and a good estimate of the peak of discharge events.

6.3 The model structures

LGSI uses a relation with the amount of water stored in the saturated zone to calculate discharge fluxes. LGSI is a lumped hydrological model, but it does include spatially variable processes (Van der Velde, 2011). Based on the findings in Chapter 5 it seems that the underestimating of peaks at lower time discretization is of less importance using this relation with water stored in the saturated zone. Because the concepts of LGSI are based on very accurate distributed MODFLOW simulations, the contribution of each flow route can be modelled very accurately only based on soil moisture levels.

Quick flow routes, like overland flow, are important to be simulated correctly for flash floods. Overland flow is an important contribution to the total outflow of a catchment. However, often it is assumed rainwater will infiltrate in the soil and flow to the surface water system via the underground (Rozemeijer and Van der Velde, 2008). In HBV, Wageningen Model and SAC-SMA this surface runoff will only occur when the soil has reached saturation. But during extreme rainfall events precipitation rates may exceed the infiltration rate causing ponding and overland flow long before complete saturation of the soil has occurred. This implementation of overland flow might result in underestimating of discharge peaks.

Although the definition of each discharge component is not consistent between the models, from Figure 5.5 and 5.6 it is clear LGSI has the least contribution of baseflow during the simulation period. The absence of significant slopes makes groundwater the dominant contributor to stream discharge in the Hupsel Brook catchment for most years. The higher contribution of the quick flow components seems logical during this wet year. As Rozemeijer and Van der Velde (2008) showed, overland flow is a very important contribution to total outflow, therefore the 44 % overland flow could be valid.

6.4 Recommendations

There is some range in efficiency values found after running each model four times (Figure 4.1). Finding the global maximum on the response surface might be a difficult task which results in not finding one optimal set of parameters. An improvement could be made by using the technique described by Willems (2009). The basic difference is that the model is separately calibrated on the baseflow and on the total outflow, rather than just on the total outflow alone. After calibration on the baseflow the slow parameters can be fixed. The parameters responsible for the fast component do not play a role during the baseflow period yet. When the model is calibrated on the total outflow there are a fewer degrees of freedom. The risk of calibrating to a local optimum is decreased with this strategy. Willems (2009) also found that the physical relations are better incorporated in the model structure in this way.

7. Conclusion

In this study 5 lumped rainfall runoff models were compared in their ability to describe the discharge peak observed in the Hupsel Brook catchment on 27 August 2010. Although the total volume of discharged water in the hydrological year 2010-2011 was not the highest ever measured, the discharge peak was almost two times as high as the highest peak ever measured before, making this event very interesting for research questions. The small catchment, with a relatively shallow phreatic aquifer, responded also quickly to precipitation input (lag time = 10 hours).

The models which are compared in this study were all able to simulate the observed rise in discharge with a good accuracy (NSE > 0.6). The model with the highest efficiency for the daily time resolution was the Lowland Groundwater Surface water Interaction (LGSI) and for the hourly time resolution was the Wageningen Model. The advantage of LGSI is that the flow routes in the model are also physically measurable. The Wageningen Model gives a slow, fast and surface runoff component. To get insight in the catchment, only the distinction between a slow or fast discharge component does not give enough information to compare it to measured time series. The disadvantage of the LGSI model is that the relations between groundwater depth distributions and water fluxes has to be calculated first with a spatially distributed model.

The Soil, Water, Atmosphere, Plant (SWAP) model simulated too much evapotranspiration during summer, causing very deep groundwater levels during the period when the discharge peak occurred. A correction in Leaf Area Index (LAI) was necessary to reduce evapotranspiration values. This resulted in wetter top soils and to adjust for this the K_{sat} value was increased. The combination of adjusted LAI and K_{sat} resulted in a good fitting model (NSE = 0.769). The low transpiration values, due to the low LAI during the event, resulted in groundwater levels which stayed too long above soil surface. The chosen LAI values gave however the best fitting model based on the simulated discharge. Increasing the LAI slightly, to increase transpiration and lower groundwater levels, resulted in very low model performance. Factors which might also cause too long ponding times are the overland flow resistance (γ) and the critical ponding layer depth ($h_{0,threshold}$). When the resistance or critical ponding layer depth are too large, surface water will not runoff, and groundwater levels will remain above soil surface.

The SWAP model was calibrated on the hydrological year 01 April 2010 to 01 April 2011. The alterations in LAI did not result in good model performance for other years. The effect of the alterations in LAI depend on how wet a year is. During dry periods a lower LAI will not reduce evapotranspiration as much as during wet periods. The effect of the alteration in LAI and K_{sat} are thus not the same for different years. Since the model is very sensitive to changes in LAI, seen from the fact that a slight increase in LAI will reduce model performance significantly, other years resulted in much lower model performance.

None of the simulated soil moisture series agreed to the observed soil moisture levels. The timing of soil moisture peaks was best predicted by the Wageningen Model with a daily resolution. Though it was found the Wageningen Model does make a mistake in calculating soil moisture levels. The model uses too many iteration steps to calculate soil moisture, causing high soil moisture levels to be averaged out. Because of that, soil moisture levels never exceed the saturation level, and surface runoff will never occur.

The specific questions the model has to answer largely determine how high the time resolution has to be. If total water volumes during longer periods are calculated, models with a daily time resolution were also able to give reliable results. For exact timing of discharge peaks models with an hourly time resolution are preferred, because the catchment reacts fast. The lag time is only 10 hours, a model with a daily time resolution will be to coarse to analyse the exact behaviour of discharge, soil moisture and groundwater levels around the event.

The model with the lowest amount of parameters, the Wageningen Model, could simulate the timing and peak observed on 27 August best. SWAP was the model with the most parameters, but was not the best performing model. It also needed the most time to get the model working. This validates the view of Beven (1996), who said model performance might not increase with increasing model complexity.

References

Allen, R. G., Pereira, L. S., Reas, D., and Smith, M.: Crop evapotranspiration - Guidelines for computing crop water requirements FAO, Rome, 1998.

Andrews, F. T., Croke, B. F. W., and Jakeman, A. J.: An open software environment for hydrological model assessment and development, Environmental Modelling and Software, 26, 1171-1185, 2011.

Beven, K. J.: A discussion of distributed hydrological modelling, in: Distributed Hydrological Modelling, edited by: Refsgaard, J. C., and Abbott, M. B., Kluwer, Dordrecht, 255-278, 1996.

Black, T. A., Gardner, W. R., and Thurtel, G. W.: The prediction of evaporation, drainage and soil water storage for a bare soil, Soil Science Society of America Journal, 33, 655-660, 1969.

Braden, H.: Ein Energiehaushalts- und Verdunstungsmodell für Wasser- und Stoffhaushaltsuntersuchungen landwirtschaftlich genutzter Einzugsgebiete, Mitteilungen der Deutschen Bodenkundlichen Gesellschaft, 42, 294-299, 1985.

Brauer, C. C., Teuling, A. J., Overeem, A., van der Velde, Y., Hazenberg, P., Warmerdam, P. M. M., and Uijlenhoet, R.: Anatomy of extraordinary rainfall and flash flood in a Dutch lowland catchment, Hydrol. Earth Syst. Sci., 15, 1991-2005, 10.5194/hess-15-1991-2011, 2011.

Burnash, R. J. C.: The NWS river forecast system - Catchment modeling, in: Computer models of watershed hydrology, edited by: Singh, V. P., Water Resources Publications, Highlands Ranch, Colorado, U.S.A., 311-366, 1995.

Byrd, R., Lu, P., Nocedal, J., and Zhu, C.: A Limited Memory Algorithm for Bound Constrained Optimization, SIAM Journal on Scientific Computing, 16, 1190-1208, 1995.

Chen, T. H., Henderson-Sellers, A., Milly, P. C. D., Pitman, A. J., Beljaars, A. C. M., Polcher, J., Abramopoulos, F., Boone, A., Chang, S., Chen, F., Dai, Y., Desborough, C. E., Dickinson, R. E., Dümenil, L., Ek, M., Garratt, J. R., Gedney, N., Gusev, Y. M., Kim, J., Koster, R., Kowalczyk, E. A., Laval, K., Lean, J., Lettenmaier, D., Liang, X., Mahfouf, J. F., Mengelkamp, H. T., Mitchell, K., Nasonova, O. N., Noilhan, J., Robock, A., Rosenzweig, C., Schaake, J., Schlosser, C. A., Schulz, J. P., Shao, Y., Shmakin, A. B., Verseghy, D. L., Wetzel, P., Wood, E. F., Xue, Y., Yang, Z. L., and Zeng, Q.: Cabauw experimental results from the Project for Intercomparison of Land-Surface Parameterization Schemes, Journal of Climate, 10, 1194-1215, 1997.

CHRS, Hydrologic Predictions - On-Going Activities, access: 12-12-2011, 2011.

Dawson, C. W., Abrahart, R. J., and See, L. M.: HydroTest: A web-based toolbox of evaluation metrics for the standardised assessment of hydrological forecasts, Environmental Modelling and Software, 22, 1034-1052, 10.1016/j.envsoft.2006.06.008, 2007.

Eertwegh, G. A. P. H. v. d., and Meinardi, C. R.: Water- en nutriëntenhuishouding van het stroomgebied van de Hupselse Beek, RIVM, Bilthoven714901005, 138, 1999.

Feddes, R. A., Kowalik, P. J., and Zaradny, H.: Simulation of field water use and crop yield., Simulation Monographs, Wageningen, 189 pp., 1978.

Feddes, R. A.: Crop factors in relation to Makkink reference crop evapotranspiration, Evaporation and weather, 33-46, 1987.

Franchini, M., Galeati, G., and Berra, S.: Global optimization techniques for the calibration of conceptual rainfall-runoff models, Hydrological Sciences Journal, 43, 443-458, 1998.

Gaume, E., Bain, V., Bernardara, P., Newinger, O., Barbuc, M., Bateman, A., Blaškovičová, L., Blöschl, G., Borga, M., Dumitrescu, A., Daliakopoulos, I., Garcia, J., Irimescu, A., Kohnova, S., Koutroulis, A., Marchi, L., Matreata, S., Medina, V., Preciso, E., Sempere-Torres, D., Stancalie, G., Szolgay, J., Tsanis, I., Velasco, D., and Viglione, A.: A compilation of data on European flash floods, Journal of Hydrology, 367, 70-78, 2009.

Hobbelt, L.: Extreme neerslag en overstromingen in Oost-Nederland en delen van Duitsland, BSc, Hydrology and Quantitative Water Management Group, Wageningen University, Wageningen, 37 pp., 2011.

Krause, P., Boyle, D. P., and Bäse, F.: Comparison of different efficiency criteria for hydrological model assessment, Advances in Geosciences, 5, 89-97, 2005.

Kroes, J. G., Van Dam, J. C., Groenendijk, P., Hendriks, R. F. A., and Jacobs, C. M. J.: SWAP version 3.2. Theory description and user manual., Alterra Research Institute, Wageningen,Report 1649, 262 pp., 2008.

Lennartz, B., Tiemeyer, B., de Rooij, G., and Doležal, F.: Artificially drained catchments-from monitoring studies towards management approaches, Vadose Zone Journal, 9, 1-3, 2010.

Metselaar, K., Uijlenhoet, R., Teuling, R., and Brauer, C. C.: Water Quality and Quantity [Voortzetting Water], Wageningen University, Wageningen, 2011.
Morales, J. L., and Nocedal, J.: Remark on "algorithm 778: L-BFGS-B: Fortran subroutines for large-scale bound constrained optimization", ACM Transactions on Mathematical Software, 38, 2011.
Moriasi, D. N., Arnold, J. G., Van Liew, M. W., Bingner, R. L., Harmel, R. D., and Veith, T. L.: Model evaluation guidelines for systematic quantification of accuracy in watershed simulations, Transactions of the ASABE, 50, 885-900, 2007.
Nash, J. E., and Sutcliffe, J. V.: River flow forecasting through conceptual models part I - A discussion of principles, Journal of Hydrology, 10, 282-290, 1970.
Nelder, J. A., and Mead, R.: A Simplex Method for Function Minimization, The Computer Journal, 7, 308-313, 1965.
NOS, Waterschade België zeker 180 miljoen, access: 01-12-2011, 2011.
Noto, L. V., Ivanov, V. Y., Bras, R. L., and Vivoni, E. R.: Effects of initialization on response of a fully-distributed hydrologic model, Journal of Hydrology, 352, 107-125, 10.1016/j.jhydrol.2007.12.031, 2008.
Punch, W. F.: How effective are multiple populations in genetic programming, Genetic Programming, Proceedings of the Third Annual Conference, University of Wisconsin, Madison, San Francisco, CA, 1998, 308-313,
Pushpalatha, R., Perrin, C., Moine, N. L., and Andréassian, V.: A review of efficiency criteria suitable for evaluating low-flow simulations, Journal of Hydrology, 420-421, 171-182, 10.1016/j.jhydrol.2011.11.055, 2012.
Reusser, D. E., Blume, T., Schaefli, B., and Zehe, E.: Analysing the temporal dynamics of model performance for hydrological models, Hydrology and Earth System Sciences, 13, 999-1018, 2009.
Rozemeijer, J. C., and Van der Velde, Y.: Oppervlakkige afstroming ook van beland in het vlakke Nederland, H2O, 19, 88-90, 2008.
Seibert, J.: Estimation of parameter uncertainty in the HBV model, Nordic Hydrology, 28, 247-262, 1997.
Seibert, J.: Regionalisation of parameters for a conceptual rainfall-runoff model, Agricultural and Forest Meteorology, 98-99, 279-293, 1999.
Seibert, J.: Multi-criteria calibration of a conceptual runoff model using a genetic algorithm, Hydrology and Earth System Sciences, 4, 215-224, 2000.
Skaggs, R. W., Breve, M. A., and Gilliam, J. W.: Hydrologic and water quality impacts of agricultural drainage, Critical Reviews in Environmental Science and Technology, 24, 1-32, 1994.
Stricker, J. N. M., and Warmerdam, P. M. M.: ESTIMATION OF THE WATERBALANCE IN THE HUPSELSE BEEK BASIN OVER A PERIOD OF THREE YEARS AND A FIRST EFFORT TO SIMULATE THE RAINFALL-RUNOFF PROCESS FOR A COMPLETE YEAR, in: Proceedings of the International Symposium on Hydrological Research Basins and Their Use in Water Resources Planning, Bern, Switzerland, 1982, 79-388,
Talei, A., and Chua, L. H. C.: Influence of lag time on event-based rainfall-runoff modeling using the data driven approach, Journal of Hydrology, 438-439, 223-233, 2012.
Van Dam, J. C.: Field-scale water flow and solute transport. SWAP model concepts, parameter estimation, and case studies., PhD-thesis, Hydrology and Quantitative Water Management Group, Wageningen University, Wageningen, 167 pp., 2000.
Van Dam, J. C., Groenendijk, P., Hendriks, R. F. A., and Kroes, J. G.: Advances of modeling water flow in variably saturated soils with SWAP, Vadose Zone Journal, 7, 640-653, 2008.
Van der Velde, Y., De Rooij, G. H., and Torfs, P. J. J. F.: Catchment-scale non-linear groundwater-surface water interactions in densely drained lowland catchments, Hydrology and Earth System Sciences, 13, 1867-1885, 2009.
Van der Velde, Y., Rozemeijer, J. C., de Rooij, G. H., van Geer, F. C., and Broers, H. P.: Field-scale measurements for separation of catchment discharge into flow route contributions, Vadose Zone Journal, 9, 25-35, 2010.
Van der Velde, Y.: Dynamics in groundwater and surface water quality, PhD-thesis, Hydrology and Quantitative Water Management Group Wageningen University, Wageningen, 176 pp., 2011.
Van der Velde, Y., Rozemeijer, J. C., De Rooij, G. H., Van Geer, F. C., Torfs, P. J. J. F., and De Louw, P. G. B.: Improving catchment discharge predictions by inferring flow route contributions from a nested-scale monitoring and model setup, Hydrology and Earth System Sciences, 15, 913-930, 2011.
Van Loon, A. F., and Van Lanen, H. A. J.: A process-based typology of hydrological drought, Hydrol. Earth Syst. Sci. Discuss., 8, 11413-11483, 10.5194/hessd-8-11413-2011, 2011.
Velner, R., Moorman, J., and Warmerdam, P. M. M.: Neerslagafvoerrelaties solide basis voor keuzen in het hoogwaterbeheer, H2O, 41, 36-39, 2008.

Von Hoyningen-Huene, J.: Die interzeption des Niederschlages in landwirtschaftlichen Pflanzenbeständen., in: Einfluß der Landnutzung auf den Gebietswasserhaushalt, 57, Verlag Paul Parey, Hamburg und Berlin, 1-66, 1983.

Whitley, D.: A genetic algorithm tutorial, Statistics and Computing, 4, 65-85, 1994.

Willems, P.: A time series tool to support the multi-criteria performance evaluation of rainfall-runoff models, Environmental Modelling and Software, 24, 311-321, 2009.

Wösten, J. H. M., Veerman, G. J., and Stolte, J.: Water retention and hydraulic conductivity functions of top- and subsoils in The Netherlands: The Staring series., Winand Staring Centre, Wageningen, 66 pp., 1994.

Wösten, J. H. M., Veerman, G. J., De Groot, W. J. M., and Stolte, J.: Water retention and hydraulic conductivity functions of top- and subsoils in The Netherlands: The Staring series., Wageningen, 86 pp., 2001.

Appendices

Appendix A Calibrated model parameters HBV, Wag., SAC-SMA

Table 0.1 Parameter values used in HBV. The run with underscore gave the best model result.

Parameter	Run 1	Run 2	Run 3	Run 4	Unit
TT	-0.62	0.90	0.90	0.90	°C
CFMAX	2.21	9.13	8.83	9.32	mm $°C^{-1}$ d^{-1}
SFCF	1.07	0.58	0.57	0.57	-
CFR	0.09	0.06	0.04	0.05	-
CWH	0.20	0.00	0.01	0.03	-
FC	266.17	181.80	183.63	186.12	mm
Lp	0.86	0.57	0.59	0.62	-
BETA	5.44	3.68	3.81	3.98	-
PERC	1.76	1.48	1.60	1.76	mm d^{-1}
UZL	8.15	8.24	8.70	8.47	mm
K0	0.23	0.23	0.23	0.20	d^{-1}
K1	0.29	0.27	0.29	0.30	d^{-1}
K2	0.10	0.10	0.10	0.10	d^{-1}
MAXBAS	1.72	1.68	1.70	1.69	d

Table 0.2 Parameter values used in SAC-SMA. The run with underscore gave the best model result.

Parameter	Run 1	Run 2	Run 3	Run 4	Unit
UZTWM	114.97	150.00	148.95	49.59	mm
UZFWM	142.06	134.70	83.94	83.28	mm
UZK	0.44	0.44	0.42	0.36	d^{-1}
PCTIM	0.01	0.01	0.00	0.00	-
ADIMP	0.04	0.05	0.08	0.07	-
ZPERC	179.95	195.14	236.28	37.12	-
REXP	4.80	2.83	2.41	2.86	-
LZTWM	95.38	43.43	115.80	125.63	mm
LZFSM	103.91	25.72	68.94	54.86	mm
LSFPM	74.19	87.36	31.59	107.86	mm
LZSK	0.01	0.24	0.01	0.25	d^{-1}
LZPK	0.25	0.01	0.25	0.01	d^{-1}
PFREE	0.18	0.53	0.10	0.09	-

Table 0.3 Parameter values used in the Wageningen Model with daily time scale. The run with underscore gave the best model result.

Parameter	Run 1	Run 2	<u>Run 3</u>	Run 4	Unit
FC	106.08	110.44	123.97	104.65	mm
SAT	204.96	207.94	213.97	202.31	mm
REPA	1.20	1.20	1.13	1.20	-
FOS	1.87	2.31	0.34	1.88	mm d^{-2}
CR	7.20	7.51	9.99	7.17	mm^{-1}
Kf	0.10	0.10	0.10	0.10	d
Ks	120.13	102.74	76.75	120.88	d
SM0	119.83	121.23	123.01	119.52	mm
Gstore0	40.10	40.64	41.05	41.13	mm
Q_slow0	0.02	0.00	0.89	0.00	mm d^{-1}
Q_fast0	0.00	0.20	0.50	0.00	mm d^{-1}

Table 0.4 Parameter values used in the Wageningen Model with hourly time scale. The run with underscore gave the best model result.

Parameter	Run 1	Run 2	Run 3	<u>Run 4</u>	Unit
FC	89.61	90.64	91.95	88.74	mm
SAT	220.00	222.20	225.50	217.80	mm
REPA	0.98	0.99	1.00	0.97	-
FOS	0.01	0.01	0.01	0.01	mm h^{-2}
CR	10.00	9.94	9.99	10.00	mm^{-1}
Kf	18.38	18.49	18.65	18.24	h
Ks	1200.00	1211.96	1229.96	1200.00	h
SM0	120.00	121.20	123.00	118.80	mm
Gstore0	40.00	40.40	41.00	39.60	mm
Q_slow0	0.03	0.03	0.03	0.03	mm h^{-1}
Q_fast0	0.00	0.01	0.02	0.00	mm h^{-1}

Appendix B SWAP model parameters

Parameter	Unit	Value
GWLI	cm	-75
PONDMX	cm	0.2
RSRO	d	0.5
RSROEXP	-	1
COFRED	cm $d^{-1/2}$	0.35
RSIGNI	cm d^{-1}	0.5
Qbottom	cm d^{-1}	0
RDS	cm	200
KDIF	-	0.75
KDIR	-	0.75
LAI	-	range
CF	-	0.9-1
HLIM1	cm	-10
HLIM2U	cm	-25
HLIM2L	cm	-25
HLIM3H	cm	-200
HLIM3L	cm	-800
HLIM4	cm	-8000
ADCRH	cm d^{-1}	0.5
ADCRL	cm d^{-1}	0.1
DTMIN	d	0.000001
DTMAX	d	0.2

Parameter	Unit	Value
GWLCONV	cm	100
CritDevh1Cp	-	0.01
CritDevh2Cp	cm	0.1
CritDevHPondDt	cm	0.0001
MaxIt	-	30
MaxBackTr	-	3
COFAB	cm	0.25
PFREE	-	0.9
PSTEM	-	0.05
SCANOPY	cm	0.4
AVPREC	cm	6
AVEVAP	cm	1.5
RD	cm	30
RDensity		1
KY	-	1
LM2	m	14.5/300
SHAPE	-	0.5
WETPER	cm	18.84/300
ZBOTDR	cm	-80
ENTRES	d	35/20
KHTOP	cm d^{-1}	25

Mualem - van Genuchten parameters

ISOILLAY1	ORES	OSAT	ALFA	NPAR	KSAT	LEXP	ALFAW	H_ENPR	KSATEXM
1	0.01	0.43	0.0227	1.548	9.65	-0.983	0.0454	0	9.65/23.41
2	0.02	0.38	0.0214	2.075	15.56	0.039	0.0428	0	15.56
Unit	**cm^3 cm^{-3}**	**cm^3 cm^{-3}**	**cm^{-1}**	**-**	**cm d^{-1}**	**-**	**cm^{-1}**	**cm**	**cm d^{-1}**

Appendix C Graphs of time series of all variables in each model

HBV

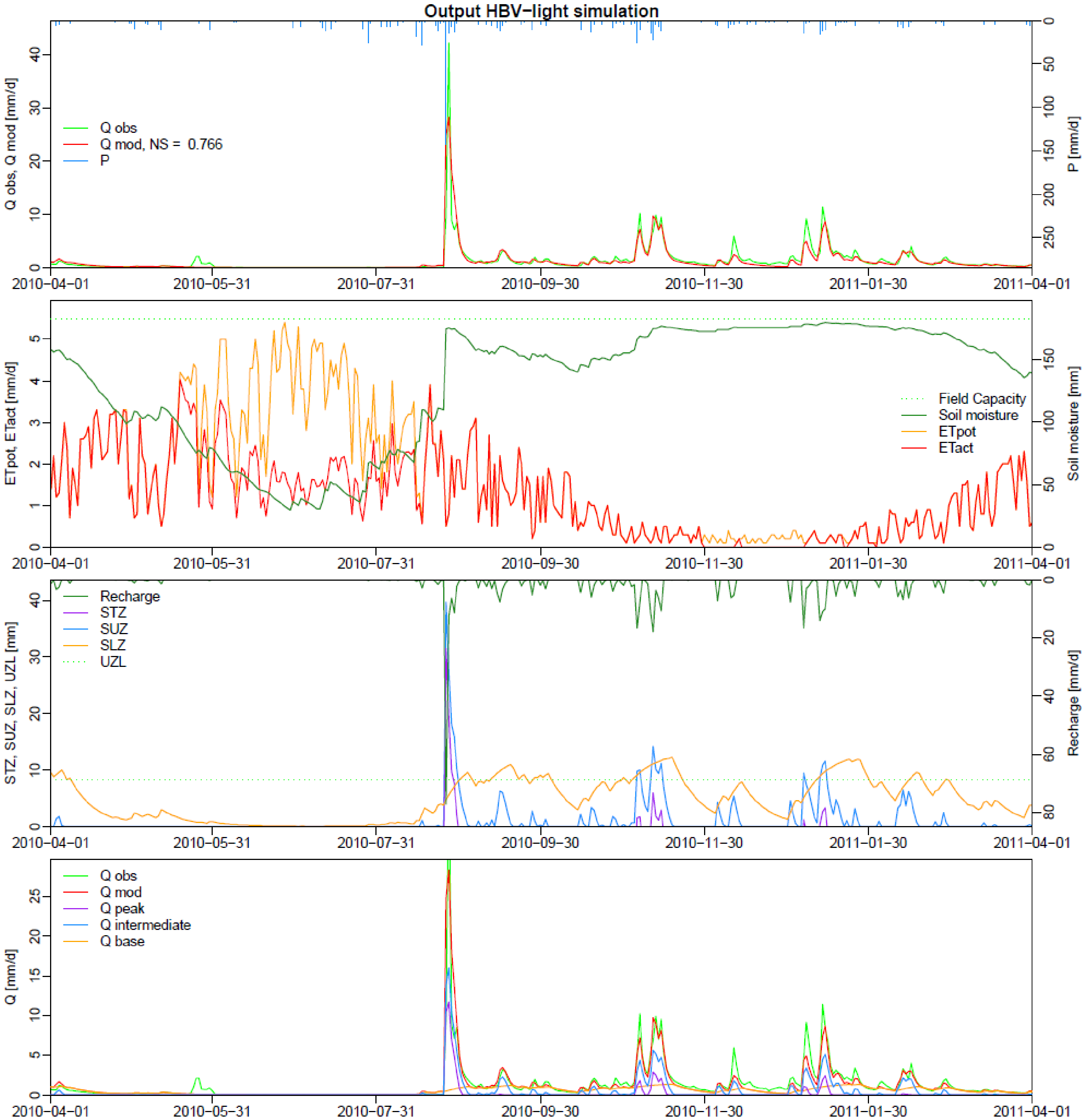

Wageningen

Output Wageningen simulation

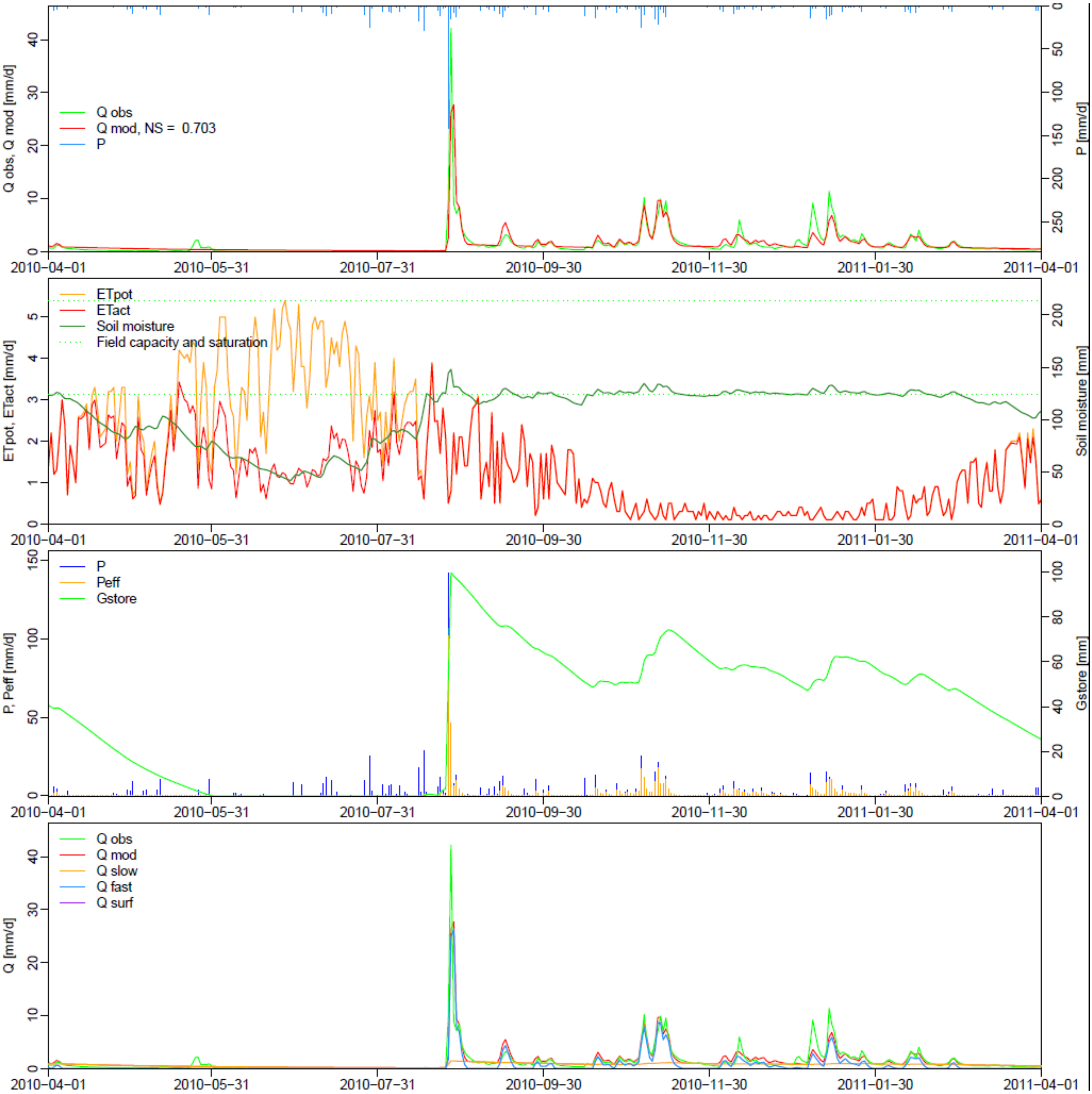

SAC-SMA

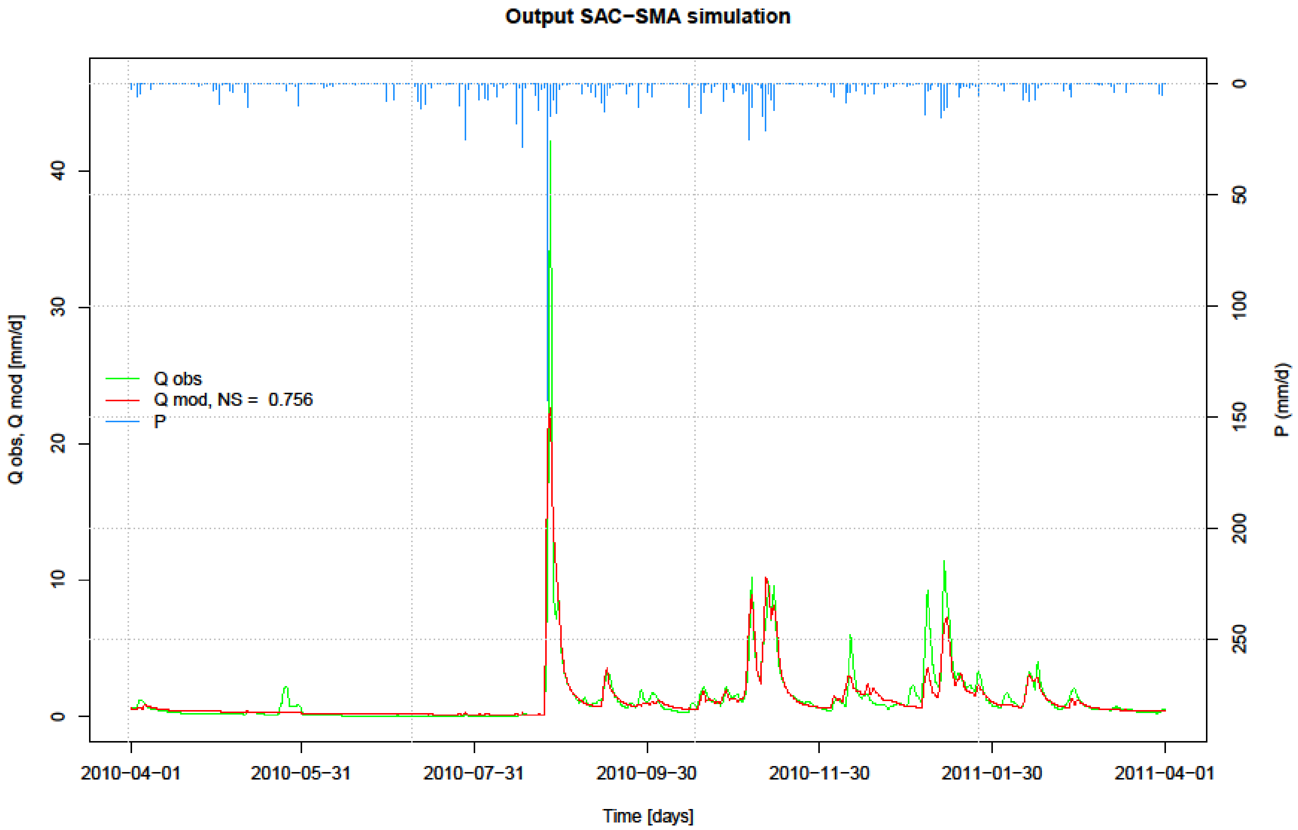

Output SAC−SMA simulation
Q obs
Q mod, NS = 0.756
P
Q obs, Q mod [mm/d]
0
10
20
30
40
P (mm/d)
0
50
100
150
200
250
2010−04−01
2010−05−31
2010−07−31
2010−09−30
2010−11−30
2011−01−30
2011−04−01
Time [days]

LGSI

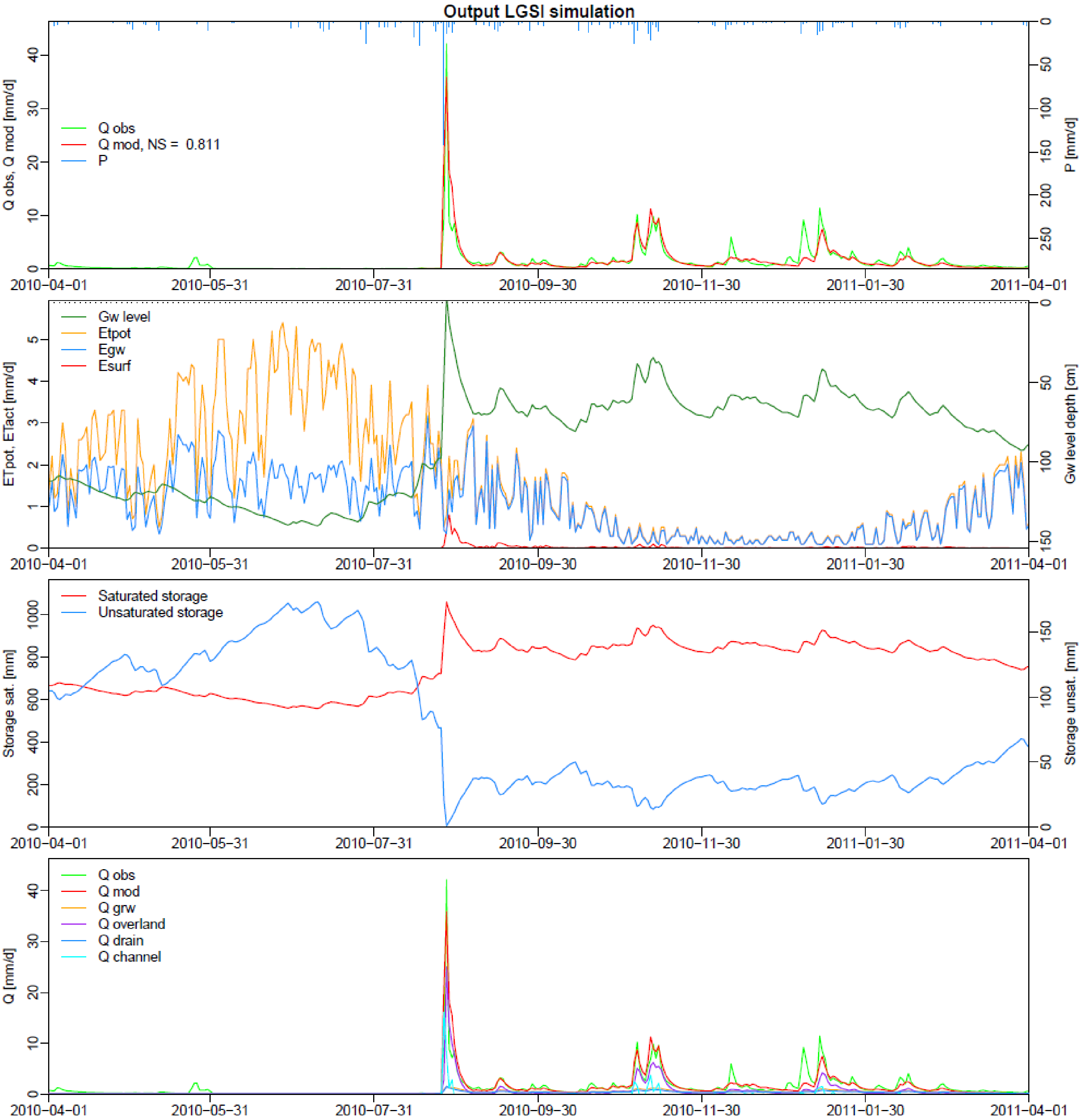

Output LGSI simulation
Q obs
Q mod, NS = 0.811
P
Q obs, Q mod [mm/d]
P [mm/d]
Gw level
Etpot
Egw
Esurf
ETpot, ETact [mm/d]
Gw level depth [cm]
Saturated storage
Unsaturated storage
Storage sat. [mm]
Storage unsat. [mm]
Q obs
Q mod
Q grw
Q overland
Q drain
Q channel
Q [mm/d]
2010−04−01
2010−05−31
2010−07−31
2010−09−30
2010−11−30
2011−01−30
2011−04−01

SWAP

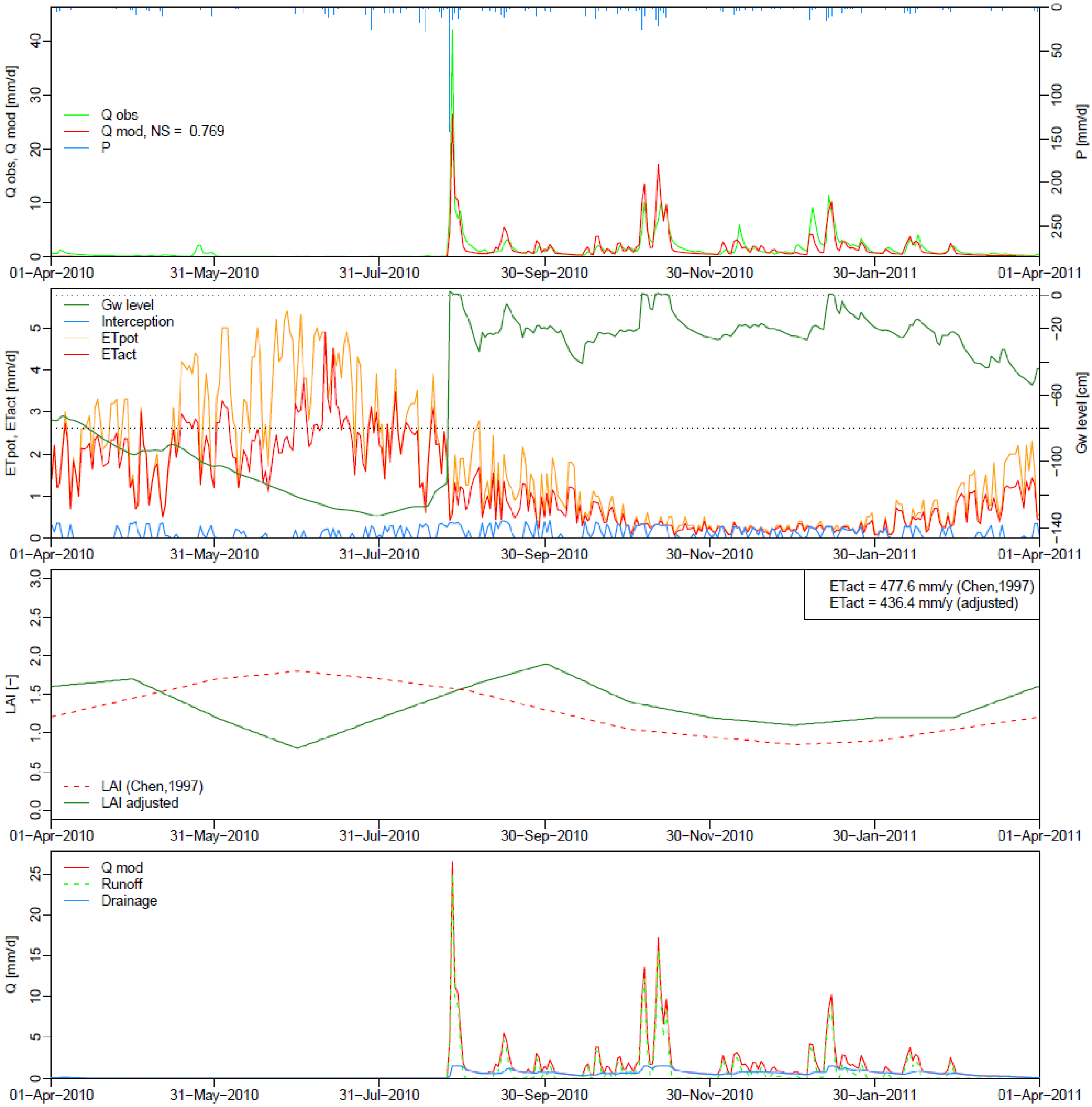
Q obs
Q mod, NS = 0.769
P
Q obs, Q mod [mm/d]
P [mm/d]
Gw level
Interception
ETpot
ETact
ETpot, ETact [mm/d]
Gw level [cm]
ETact = 477.6 mm/y (Chen,1997)
ETact = 436.4 mm/y (adjusted)
LAI [-]
LAI (Chen,1997)
LAI adjusted
Q mod
Runoff
Drainage
Q [mm/d]
01–Apr–2010
31–May–2010
31–Jul–2010
30–Sep–2010
30–Nov–2010
30–Jan–2011
01–Apr–2011

Wageningen hour

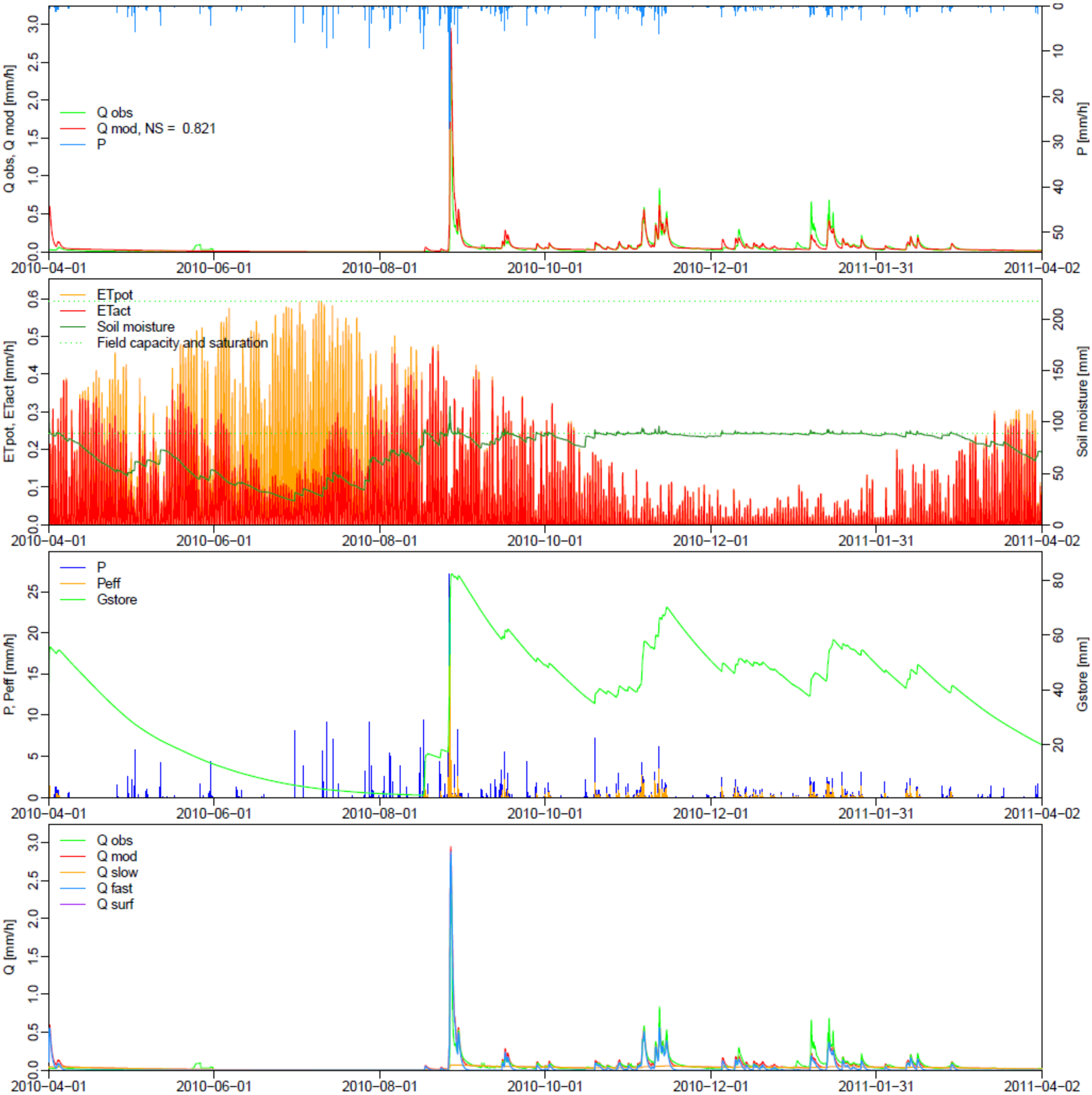

SWAP hour

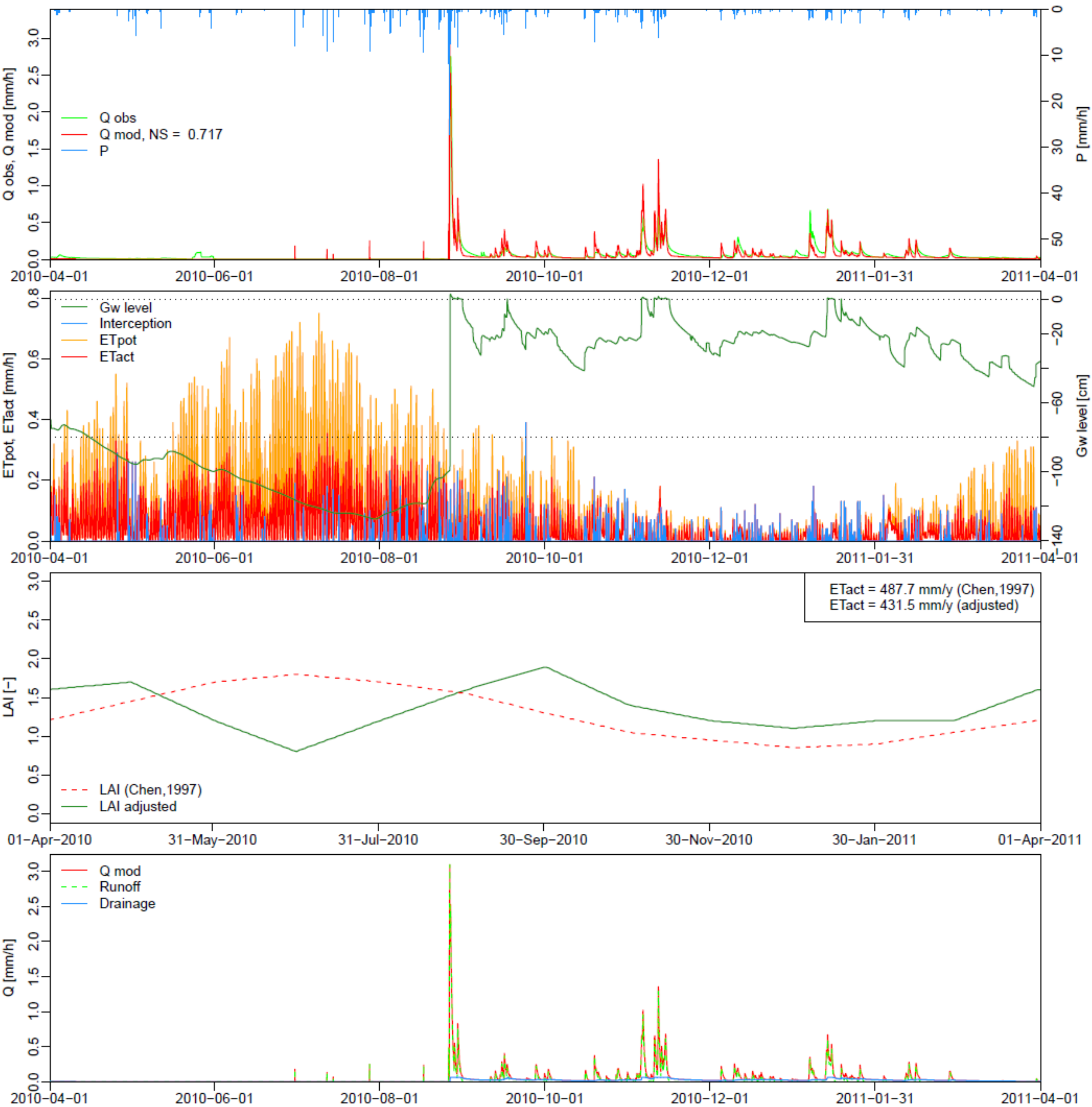
Q obs
Q mod, NS = 0.717
P
Q obs, Q mod [mm/h]
P [mm/h]
Gw level
Interception
ETpot
ETact
ETpot, ETact [mm/h]
Gw level [cm]
ETact = 487.7 mm/y (Chen,1997)
ETact = 431.5 mm/y (adjusted)
LAI (Chen,1997)
LAI adjusted
LAI [-]
01-Apr-2010
31-May-2010
31-Jul-2010
30-Sep-2010
30-Nov-2010
30-Jan-2011
01-Apr-2011
Q mod
Runoff
Drainage
Q [mm/h]
2010-04-01
2010-06-01
2010-08-01
2010-10-01
2010-12-01
2011-01-31
2011-04-01